

Nonlinear and Adaptive Frame Approximation Schemes for Elliptic PDEs: Theory and Numerical Experiments *

Stephan Dahlke, Massimo Fornasier, Miriam Primbs,
Thorsten Raasch, and Manuel Werner

Abstract

This paper is concerned with adaptive numerical frame methods for elliptic operator equations. We show how specific non-canonical frame expansions on domains can be constructed. Moreover, we study the approximation order of best n -term frame approximation which serves as the benchmark for the performance of adaptive schemes. We also discuss numerical experiments for second order elliptic boundary value problems in polygonal domains where the discretization is based on recent constructions of boundary adapted wavelet bases on the interval.

AMS subject classification: 41A46, 42C15, 42C40, 46E35, 65F20

Key Words: Adaptive algorithms, nonlinear approximation, operator equations, boundary value problems, optimal computational complexity, frames, Besov spaces, biorthogonal wavelets

1 Introduction

In recent years, wavelet methods have become a very powerful mathematical tool with many important applications, e.g., in the fields of signal analysis and numerical analysis. In signal/image analysis/compression, wavelet schemes are well-established by now, and very often they outperform other classical methods. In numerical analysis, the most exciting results have been obtained in the context of the numerical treatment of elliptic operator equations. Indeed, the strong analytical properties of wavelets yield uniformly bounded condition numbers of the associated stiffness matrices, they allow for very efficient compression strategies, and, moreover, they can be used to derive *adaptive* numerical schemes that are guaranteed to converge with optimal order [3, 10, 17]. However, due to a serious bottleneck, these impressive advantages of wavelet methods have not been fully exploited yet. Usually, the operator equation is defined on a bounded domain or on a closed manifold, and therefore a wavelet basis on this domain is needed. Although there exist by now several constructions [5, 13, 25, 26, 30, 32], none of them seems to be fully satisfying for the following reasons: one is usually faced with relatively high condition numbers, very often the

*The work of the first, fourth, and last author was supported through DFG, Grants Da 360/4-3, and Da 360/7-1. The second author acknowledges the financial support provided by the European Union's Human Potential Programme under contract MOIF-CT-2006-039438. The third author was supported through DFG, Grant Pr 1044/2-1.

wavelet basis is not smooth enough, and last, but not least, all the existing constructions are not easy to implement. One approach to ameliorate these problems is to use a weaker concept, i.e., to work with *frames* instead of bases [18, 38]. Indeed, contrary to the basis case, the construction of a smooth wavelet frame is quite easy. One only has to construct an overlapping partition of the domain by means of parametric images of the unit cube. Then, by lifting tensor product boundary adapted wavelet bases on the unit cube to each subdomain and collecting everything together, indeed a wavelet frame is obtained. Fortunately, in recent studies, it has been shown that all the advantages of wavelet methods outlined above can also be established in the case of frames [7, 18, 19, 38].

However, there are still some open problems left as we shall now explain. It has turned out that the so-called *Gelfand frames* are the right and suitable tool for numerical purposes, see Section 3. Roughly speaking, a Gelfand frame is a Hilbert frame that in addition induces norm equivalences for associated smoothness spaces. These norm equivalences are usually stated by means of expansion with respect to the canonical dual frame. However, for wavelet frames constructed as described above, the sufficient properties (e.g., smoothness and cancellation properties) of the canonical dual to establish the norm equivalence cannot be easily checked. Therefore it is clearly desirable to generalize the existing constructions to non-canonical dual frames. Indeed, in this paper, we show that such a generalization is possible, and we also present a very simple construction of a non-canonical dual system which is based on a suitable underlying partition of unity.

Another open question is concerned with optimality of adaptive wavelet frame schemes. Usually, the benchmark for adaptive schemes is best n -term approximation. In the basis case, the norm equivalences imply that this approximation order is completely determined by the regularity of the function one wants to approximate as measured in a specific scale of Besov spaces. In the case of frames, such a complete characterization cannot be expected, since due to the redundancy of the frame a Bernstein estimate often fails to hold. Nevertheless, a Jackson-type estimate can usually be shown, so that at least an upper bound for best n -term approximation can be derived. If some knowledge about the smoothness and cancellation properties of the dual frame under consideration is available, it has turned out recently that also Bernstein-type estimates can be expected, at least in the case of wavelet bi-frames on \mathbb{R}^n , see [4]. In this paper, we prove a similar result for Gelfand frame expansions of the solutions to second order elliptic operator equations defined in polygonal domains in \mathbb{R}^2 : if the solution is contained in a specific scale of Besov spaces, then there exists a Gelfand frame expansion (with respect to a non-canonical dual) such that the associated frame coefficients show the same decay as for the basis case, which implies that the best n -term frame approximation realizes the same approximation order. Consequently, an optimal adaptive wavelet frame scheme should also converge with this order, and that is what is indeed observed in practice, see Section 6.

A third important problem is concerned with concrete applications and implementations of adaptive frame schemes. As outlined above, the basic ingredient is always a suitable wavelet basis on the unit cube, and the overall performance of the algorithm directly depends on the properties of this basis. In practice, one is very often faced with the problem that, e.g., the condition numbers of the bases are not as low as desirable, especially for bases of higher order, and this drawback clearly diminishes the applicability of the whole scheme. Consequently, there is urgent need for much more stable boundary adapted wavelet bases.

Quite recently, a very promising approach has been developed in [34]. First numerical tests indeed show that the condition numbers associated with this basis are much lower compared to other existing approaches. Therefore, in this paper we explain how this new basis can be incorporated in an adaptive wavelet frame scheme, and we present numerical experiments, which confirm the quantitative improvement with respect to the basis constructed in [24].

This paper is organized as follows. In Section 2, we briefly recall the setting of adaptive wavelet frame discretizations as far as it is needed for our purposes. Then, in Section 3, we discuss the basic concept of Gelfand frames and present a quite natural construction of a non-canonical dual frame which is based on a suitable partition of unity. Section 4 is devoted to nonlinear approximation schemes based on Gelfand frames. We show that the approximation order of best n -term frame approximation that can be achieved is directly determined by the Besov smoothness of u . Then, in Section 5, we briefly recall the newly developed construction of boundary adapted wavelets. Finally, in Section 6, we shortly explain the building blocks of adaptive frame algorithms and present some numerical experiments for the Poisson equation on the L -shaped domain.

2 Frame Discretization of Elliptic Problems

In this section, we briefly describe the basic concepts of frame discretization schemes for linear elliptic operator equations

$$\mathcal{L}u = f, \tag{2.1}$$

where we will assume \mathcal{L} to be a boundedly invertible operator from some Hilbert space H into its normed dual H' , i.e.,

$$\|\mathcal{L}u\|_{H'} \approx \|u\|_H, \quad u \in H. \tag{2.2}$$

Here and in the following ‘ $a \approx b$ ’ means that both quantities can be uniformly bounded by some constant multiple of each other. Likewise, ‘ \lesssim ’ indicates inequalities up to constant factors. We write out such constants explicitly only when their values matter.

Since \mathcal{L} is boundedly invertible, (2.1) has a unique solution u for any $f \in H'$. In the sequel, we shall focus on the important special case where

$$a(v, w) := \langle \mathcal{L}v, w \rangle \tag{2.3}$$

defines a *symmetric* bilinear form on H , $\langle \cdot, \cdot \rangle$ corresponding to the dual pairing of H' and H . We will always assume that $a(\cdot, \cdot)$ is *elliptic* in the sense that

$$a(v, v) \approx \|v\|_H^2, \tag{2.4}$$

which is easily seen to imply (2.2).

Typical examples are variational formulations of second order elliptic boundary value problems on a domain $\Omega \subset \mathbb{R}^n$ such as the Poisson equation

$$\begin{aligned} -\Delta u &= f && \text{in } \Omega, \\ u &= 0 && \text{on } \partial\Omega. \end{aligned} \tag{2.5}$$

In this case, $H = H_0^1(\Omega)$, $H' = H^{-1}(\Omega)$, and the corresponding bilinear form is given by

$$a(v, w) = \int_{\Omega} \nabla v \cdot \nabla w \, dx. \quad (2.6)$$

Thus typically H is a Sobolev space. Therefore, from now on, we will always assume that H and H' , together with $L_2(\Omega)$, form a *Gelfand triple*, i.e.,

$$H \subset L_2(\Omega) \subset H' \quad (2.7)$$

with continuous and dense embeddings.

We are interested in the discretization of (2.1) using wavelet frames. To this end, recall first that a subset $\mathcal{F} = \{f_n : n \in \mathcal{N}\}$ of a Hilbert space \mathcal{H} is called a *frame* for \mathcal{H} if

$$\|f\|_{\mathcal{H}}^2 \approx \sum_{n \in \mathcal{N}} |\langle f, f_n \rangle_{\mathcal{H}}|^2, \quad \text{for all } f \in \mathcal{H}. \quad (2.8)$$

By (2.8), any frame \mathcal{F} for \mathcal{H} is automatically dense, which makes frames suitable for the numerical discretization of, e.g., the operator equation (2.1). Moreover, the analysis operator $F := F_{\mathcal{F}} : \mathcal{H} \rightarrow \ell_2(\mathcal{N})$ of a frame \mathcal{F} , $F_{\mathcal{F}}f = (\langle f, f_n \rangle_{\mathcal{H}})_{n \in \mathcal{N}}$, and the synthesis operator $F^* : \ell_2(\mathcal{N}) \rightarrow \mathcal{H}$, $F^*\mathbf{c} = \sum_{n \in \mathcal{N}} c_n f_n =: \mathbf{c}^{\top} \mathcal{F}$ are bounded. The frame operator $S := F^*F$ is positive and boundedly invertible on \mathcal{H} , so that every $f \in \mathcal{H}$ possesses the non-orthogonal expansions

$$f = SS^{-1}f = \sum_{n \in \mathcal{N}} \langle f, S^{-1}f_n \rangle_{\mathcal{H}} f_n = S^{-1}Sf = \sum_{n \in \mathcal{N}} \langle f, f_n \rangle_{\mathcal{H}} S^{-1}f_n. \quad (2.9)$$

The set $\tilde{\mathcal{F}} = \{S^{-1}f_n : n \in \mathcal{N}\}$ is again a frame for \mathcal{H} , the so-called *canonical dual frame* with associated analysis operator $F_{\tilde{\mathcal{F}}}$. In general, there exist many possible dual frames $\{\tilde{f}_n : n \in \mathcal{N}\} \subset \mathcal{H}$ such that

$$f = \sum_{n \in \mathcal{N}} \langle f, \tilde{f}_n \rangle_{\mathcal{H}} f_n = \sum_{n \in \mathcal{N}} \langle f, f_n \rangle_{\mathcal{H}} \tilde{f}_n \quad (2.10)$$

with the norm equivalence $\|f\|_{\mathcal{H}} \approx \|F_{\tilde{\mathcal{F}}}f\|_2$, but their construction might be less obvious. A frame \mathcal{F} is a Riesz basis for \mathcal{H} if and only if $\ker(F^*) = \{0\}$ and in such a case the dual is uniquely determined.

Concerning the discretization of (2.1), it remains to specify a suitable frame \mathcal{F} for the solution space H . Here we are particularly interested in the class of wavelet frames. Due to the fact that wavelet systems are typically constructed in L_2 rather than in the solution space H , we will consider frames that simultaneously allow expansions of the form (2.10) in a Hilbert space \mathcal{H} and in a densely embedded Hilbert space $\mathcal{X} \subset \mathcal{H}$. Here it is

$$\mathcal{X} \subset \mathcal{H} \simeq \mathcal{H}' \subset \mathcal{X}', \quad (2.11)$$

such that $(\mathcal{X}, \mathcal{H}, \mathcal{X}')$ is a *Gelfand triple*. Frames tailored to this Gelfand triple situation are given by the class of Gelfand frames, as introduced in [18]. A frame \mathcal{F} for \mathcal{H} with dual

frame $\tilde{\mathcal{F}}$ is a *Gelfand frame* for the Gelfand triple $(\mathcal{X}, \mathcal{H}, \mathcal{X}')$, if $\mathcal{F} \subset \mathcal{X}$, $\tilde{\mathcal{F}} \subset \mathcal{X}'$ and there exists a Gelfand triple $(b, \ell_2(\mathcal{N}), b')$ of sequence spaces such that

$$F^* : b \rightarrow \mathcal{X}, F^* \mathbf{c} = \mathbf{c}^\top \mathcal{F} \quad \text{and} \quad \tilde{F} : \mathcal{X} \rightarrow b, \tilde{F} f = (\langle f, \tilde{f}_n \rangle_{\mathcal{X} \times \mathcal{X}'})_{n \in \mathcal{N}} \quad (2.12)$$

are bounded operators. By duality, also the operators

$$\tilde{F}^* : b' \rightarrow \mathcal{X}', \tilde{F}^* \mathbf{c} = \mathbf{c}^\top \tilde{\mathcal{F}} \quad \text{and} \quad F : \mathcal{X}' \rightarrow b', F f = (\langle f, f_n \rangle_{\mathcal{X}' \times \mathcal{X}})_{n \in \mathcal{N}} \quad (2.13)$$

are bounded. In particular, the following reproducing formulas hold

$$f = \sum_n \langle f, \tilde{f}_n \rangle_{\mathcal{X} \times \mathcal{X}'} f_n \quad \text{for all } f \in \mathcal{X} \quad (2.14)$$

$$g = \sum_n \langle g, f_n \rangle_{\mathcal{X}' \times \mathcal{X}} \tilde{f}_n \quad \text{for all } g \in \mathcal{X}'. \quad (2.15)$$

In the following, we will assume that the sequence spaces b and $\ell_2(\mathcal{N})$ can be identified via an isomorphism $D : b \rightarrow \ell_2(\mathcal{N})$. As a consequence, the system $D^{-1}\mathcal{F}$ is indeed a frame for \mathcal{X} , see [35] for a proof. In all cases of practical interest, the sequence spaces b will turn out to be suitable weighted $\ell_2(\mathcal{N})$ -spaces.

For the applications we have in mind, clearly the case $(\mathcal{X}, \mathcal{H}, \mathcal{X}') = (H, L_2(\Omega), H')$, where H denotes some Sobolev space, is the most important one. One prominent example [5, 23, 24, 25, 26, 30, 40] of a Gelfand frame is any wavelet Riesz basis $\Psi = \{\psi_\lambda : \lambda \in \mathcal{I}\}$ in $L_2(\Omega)$, $\Omega \subset \mathbb{R}^n$, such that a range $s \in (-\tilde{\gamma}, \gamma)$ of Sobolev spaces $H_0^s(\Omega)$ can be characterized by weighted sequence norms of the primal wavelet coefficient arrays

$$\|f\|_{H^s(\Omega)} \approx \left(\sum_{\lambda \in \mathcal{I}} 2^{2|\lambda|s} |\langle f, \tilde{\psi}_\lambda \rangle_{L_2(\Omega)}|^2 \right)^{1/2}, \quad f \in H_0^s(\Omega). \quad (2.16)$$

Here we have used that for wavelet systems, the scale mapping $\lambda \mapsto |\lambda| \in \mathbb{Z}_{\geq j_0}$ is well-defined. Any such wavelet Riesz basis Ψ is a Gelfand frame for $(H_0^s(\Omega), L_2(\Omega), H^{-s}(\Omega))$ for $s \in (-\tilde{\gamma}, \gamma)$, with the weighted sequence spaces $b := \ell_{2,2^s}(\mathcal{I}) := \ell_{2,2^{2|\cdot|s}}(\mathcal{I})$. Here we use the weighted ℓ_2 spaces

$$\ell_{2,w}(\mathcal{I}) := \left\{ \mathbf{c} = (c_\lambda)_{\lambda \in \mathcal{I}} : \|\mathbf{c}\|_{\ell_{2,w}(\mathcal{I})}^2 := \sum_{\lambda \in \mathcal{I}} |c_\lambda|^2 w(\lambda) < \infty \right\} \quad (2.17)$$

for some weight function $w : \mathcal{I} \rightarrow \mathbb{R}_+$.

Under the aforementioned assumptions on a Gelfand frame \mathcal{F} for $(H, L_2(\Omega), H')$, the following lemma holds [18, 38], in analogy to the case of wavelet bases.

Lemma 2.1. *Let F and F^* be the analysis and synthesis operators of a Gelfand frame \mathcal{F} associated to the Gelfand triple $(H, L_2(\Omega), H')$. Then, under the assumptions (2.3) and (2.4) on \mathcal{L} , the operator*

$$\mathbf{G} := (D^*)^{-1} F \mathcal{L} F^* D^{-1} \quad (2.18)$$

is a bounded operator from $\ell_2(\mathcal{N})$ to $\ell_2(\mathcal{N})$. Moreover $\mathbf{G} = \mathbf{G}^$, and it is boundedly invertible on its range $\text{ran}(\mathbf{G}) = \text{ran}((D^*)^{-1}F)$.*

With

$$\mathbf{f} := (D^*)^{-1} F f, \quad (2.19)$$

we are therefore left with the problem to solve

$$\mathbf{G} \mathbf{u} = \mathbf{f}, \quad (2.20)$$

because the solution u to (2.1) is obtained by the identity $u = F^* D^{-1} \mathbf{u}$ [18, 38]. It has been shown in [19, 38] that the infinite linear system (2.20) can be solved with well known iterative methods such as a damped Richardson iteration or a steepest descent scheme.

3 Gelfand Frames on Domains

3.1 The General Setting

We shall now be concerned with a straightforward construction of wavelet Gelfand frames on a bounded domain $\Omega \subset \mathbb{R}^n$ using domain decomposition arguments. To this end, we assume that Ω is the union of overlapping patches $\mathcal{C} = \{\Omega_i\}_{i=1}^m$

$$\Omega = \bigcup_{i=1}^m \Omega_i, \quad (3.1)$$

where each patch Ω_i is the image of the unit cube $\square = (0, 1)^n$ under a suitable parametrization $\Omega_i = \kappa_i(\square)$. We assume furthermore that the parametrizations κ_i are C^k -diffeomorphisms and that

$$|\det D\kappa_i(x)| \approx 1, \quad \text{for } x \in \square. \quad (3.2)$$

Clearly, the set of admissible domains Ω is restricted by raising these regularity conditions; the boundary of Ω has to be piecewise smooth enough. However, the particularly attractive case of polyhedral domains is still covered.

Given a reference wavelet Riesz basis $\Psi^\square = \{\psi_\mu : \mu \in \mathcal{I}^\square\} \subset H_0^s(\square)$ on the cube, $s > 0$, we lift the system Ψ^\square to Ω_i by setting

$$\psi_{i,\mu} := \frac{\psi_\mu^\square(\kappa_i^{-1}(\cdot))}{|\det D\kappa_i(\kappa_i^{-1}(\cdot))|^{1/2}}. \quad (3.3)$$

The denominator is chosen in such a way that $\|\psi_\lambda\|_{L_2(\Omega)} = \|\psi_\mu^\square\|_{L_2(\square)}$. Analogously, we also lift the dual wavelets to Ω_i :

$$\tilde{\psi}_{i,\mu} := \frac{\tilde{\psi}_\mu^\square(\kappa_i^{-1}(\cdot))}{|\det D\kappa_i(\kappa_i^{-1}(\cdot))|^{1/2}}. \quad (3.4)$$

Then it is immediate to see that the system $\Psi^{(i)} := \{\psi_{i,\mu} : \mu \in \mathcal{I}^\square\}$ is a Riesz basis in $L_2(\Omega_i)$ with dual Riesz basis $\tilde{\Psi}^{(i)} := \{\tilde{\psi}_\lambda : \lambda \in \mathcal{I}^\square\}$, characterizing the corresponding scale of Sobolev spaces over Ω_i . The most simple method to derive a wavelet Gelfand frame over

the domain Ω from the local bases $\Psi^{(i)}$ is to aggregate them by means of the zero extension operators $E_i : \Omega_i \rightarrow \Omega$. Using the global index set

$$\mathcal{I} := \bigcup_{i=1}^m \{i\} \times \mathcal{I}^\square, \quad (3.5)$$

with $|\lambda| := |\mu|$ for $\lambda = (i, \mu) \in \mathcal{I}$, we will consider the family

$$\Psi := \{\psi_\lambda : \lambda \in \mathcal{I}\}, \quad \psi_{(i,\mu)} := E_i \psi_{i,\mu}, \quad \text{for } (i, \mu) \in \mathcal{I}. \quad (3.6)$$

The operators E_i being bounded from $H_0^s(\Omega_i)$ to $H_0^s(\Omega)$, we have that $\Psi \subset H_0^s(\Omega)$ for $s \geq 0$. In the following we may omit E_i and we will assume that the functions are smoothly zero-extended to all Ω . It is straightforward to see that Ψ is a frame for $L_2(\Omega)$.

Lemma 3.1. *The aggregated system Ψ from (3.6) is a frame for $L_2(\Omega)$.*

Proof. For $f \in L_2(\Omega)$, (3.2) and a transformation of coordinates imply

$$\|f\|_{L_2(\Omega_i)}^2 \approx \|f(\cdot) |\det D\kappa_i(\kappa_i^{-1}(\cdot))|^{1/2}\|_{L_2(\Omega_i)}^2 \approx \|f \circ \kappa_i(\cdot) |\det D\kappa_i(\cdot)|^{1/2}\|_{L_2(\square)}^2.$$

Inserting the frame condition for Ψ^\square in $L_2(\square)$, we get the frame condition for $\Psi^{(i)}$ in $L_2(\Omega_i)$

$$\|f\|_{L_2(\Omega_i)}^2 \approx \sum_{\mu \in \mathcal{I}^\square} \left| \langle f \circ \kappa_i(\cdot) |\det D\kappa_i(\cdot)|^{1/2}, \psi_\mu^\square \rangle_{L_2(\square)} \right|^2 = \sum_{\mu \in \mathcal{I}^\square} \left| \langle f, \psi_{i,\mu} \rangle_{L_2(\Omega_i)} \right|^2. \quad (3.7)$$

Using the inequalities

$$\|f\|_{L_2(\Omega)}^2 \leq \sum_{i=1}^m \|f\|_{L_2(\Omega_i)}^2 \leq m \|f\|_{L_2(\Omega)}^2,$$

the frame condition for Ψ follows by summing up (3.7) over i . \square

Unfortunately, the global canonical dual $S^{-1}\Psi$ of the frame Ψ is only implicitly given and its properties are not obvious. In particular, it is not immediately clear how to prove the Gelfand frame properties in $(H_0^s(\Omega), L_2(\Omega), H^{-s}(\Omega))$. As an alternative, we therefore propose to work with *non-canonical* duals instead. As soon as the particular decomposition $\Omega = \bigcup_{i=1}^m \Omega_i$ admits the construction of a partition of unity $\{\sigma_i\}_{1 \leq i \leq m}$ subordinate to the patches Ω_i , i.e.,

- i) $\text{supp } \sigma_i \subset \bar{\Omega}_i$,
- ii) $\|\sigma_i u\|_{H^s(\Omega_i)} \lesssim \|u\|_{H^s(\Omega)}$ holds uniformly in $u \in H^s(\Omega)$, and
- iii) $\sigma_i u \in H_0^s(\Omega_i)$, for all $u \in H_0^s(\Omega)$, $i = 1, \dots, m$,

we can immediately specify a non-canonical global dual frame for Ψ as is shown in the following proposition, see also Subsection 4.4 of [38].

Proposition 3.2. *Let Ψ be defined as in (3.6) and assume that $\{\sigma_i\}_{i=1}^m$ is a partition of unity subordinate to the patches Ω_i . Then, with $\tilde{\psi}_{i,\mu}$ being the lifted local duals from (3.4), the system*

$$\tilde{\Psi} := \{\tilde{\psi}_\lambda : \lambda \in \mathcal{I}\}, \quad \tilde{\psi}_{(i,\mu)} := E_i(\sigma_i \tilde{\psi}_{i,\mu}), \quad \text{for } (i, \mu) \in \mathcal{I} \quad (3.8)$$

is a non-canonical global dual frame for Ψ in $L_2(\Omega)$. More specific, Ψ and $\tilde{\Psi}$ form a wavelet Gelfand frame for $(H_0^s(\Omega), L_2(\Omega), H^{-s}(\Omega))$ with respect to the Gelfand triple of sequence spaces $(\ell_{2,2^s}(\mathcal{I}), \ell_2(\mathcal{I}), \ell_{2,2^{-s}}(\mathcal{I}))$.

Proof. By the partition of unity property, it is $\|u\|_{L_2(\Omega)}^2 \approx \sum_{i=1}^m \|\sigma_i u\|_{L_2(\Omega)}^2$, which implies the frame property of $\tilde{\Psi}$ for $L_2(\Omega)$,

$$\|u\|_{L_2(\Omega)}^2 \approx \sum_{i=1}^m \sum_{\mu \in \mathcal{I}^\square} |\langle u, \sigma_i \tilde{\psi}_{i,\mu} \rangle_{L_2(\Omega_i)}|^2, \quad u \in L_2(\Omega).$$

Clearly, the validity of the duality relation (2.10) is induced by the partition property of the σ_i . Concerning the Gelfand frame property, we will show that the operators $F^* : \ell_{2,2^s}(\mathcal{I}) \rightarrow H_0^s(\Omega)$, $F^* \mathbf{c} = \mathbf{c}^\top \Psi$, and $\tilde{F} : H_0^s(\Omega) \rightarrow \ell_{2,2^s}(\mathcal{I})$, $\tilde{F} f = (\langle f, \tilde{\psi}_\lambda \rangle_{H_0^s(\Omega) \times H^{-s}(\Omega)})_{\lambda \in \mathcal{I}}$ are bounded. Note first that any sequence in $\ell_{2,2^s}(\mathcal{I})$ can be uniquely resorted as an m -tuple $\mathbf{c} = (\mathbf{c}^{(1)}, \dots, \mathbf{c}^{(m)}) \in \ell_{2,2^s}(\mathcal{I}^\square)^m$ with $c_{(i,\mu)} = c_\mu^{(i)}$ and equivalent norms

$$\|\mathbf{c}\|_{\ell_{2,2^s}(\mathcal{I})} \approx \|(\mathbf{c}^{(1)}, \dots, \mathbf{c}^{(m)})\|_{\ell_{2,2^s}(\mathcal{I}^\square)^m} := \sum_{i=1}^m \|\mathbf{c}^{(i)}\|_{\ell_{2,2^s}(\mathcal{I}^\square)}, \quad (3.9)$$

where the constants involved do not depend on s . By assumption, the local Riesz basis property of $(2^{-s|\mu|} \psi_{i,\mu})_{\mu \in \mathcal{I}^\square}$ in $H_0^s(\Omega_i)$ implies that the operators $(F^{(i)})^* : \ell_{2,2^s}(\mathcal{I}^\square) \rightarrow H_0^s(\Omega_i)$, $(F^{(i)})^* \mathbf{c} = \mathbf{c}^\top \Psi^{(i)}$, are bounded. Since the operators E_i are continuous, for any $\mathbf{c} \in \ell_{2,2^s}(\mathcal{I})$ one has the representation

$$F^* \mathbf{c} = \sum_{i=1}^m \sum_{\mu \in \mathcal{I}^\square} c_\mu^{(i)} \psi_{i,\mu} = \sum_{i=1}^m E_i (F^{(i)})^* \mathbf{c}^{(i)},$$

from which, by applying the continuity of E_i and $(F^{(i)})^*$, and by using (3.9) follows

$$\|F^* \mathbf{c}\|_{H^s(\Omega)} \leq \sum_{i=1}^m \| (F^{(i)})^* \mathbf{c}^{(i)} \|_{H^s(\Omega_i)} \lesssim \sum_{i=1}^m \|\mathbf{c}^{(i)}\|_{\ell_{2,2^s}(\mathcal{I}^\square)} \approx \|\mathbf{c}\|_{\ell_{2,2^s}(\mathcal{I})}.$$

As regards the continuity of \tilde{F} , we know that again by the Riesz basis property of $(2^{-s|\mu|} \psi_{i,\mu})_{\mu \in \mathcal{I}^\square}$ in $H_0^s(\Omega_i)$, the operators $\tilde{F}^{(i)} : H_0^s(\Omega_i) \rightarrow \ell_{2,2^s}(\mathcal{I}^\square)$, $\tilde{F}^{(i)} f = (\langle f, \tilde{\psi}_{i,\mu} \rangle_{H_0^s(\Omega_i) \times H^{-s}(\Omega_i)})_{\mu \in \mathcal{I}^\square}$, are bounded. It follows from $\text{supp } \tilde{\psi}_{(i,\mu)} \subset \bar{\Omega}_i$ that

$$\|\tilde{F} f\|_{\ell_{2,2^s}(\mathcal{I})} \approx \sum_{i=1}^m \|\tilde{F}^{(i)} f|_{\Omega_i}\|_{\ell_{2,2^s}(\mathcal{I}^\square)} \lesssim \sum_{i=1}^m \|f\|_{H^s(\Omega_i)} \lesssim \|f\|_{H^s(\Omega)}.$$

□

Thus, it remains to discuss the availability of a suitable partition of unity $\{\sigma_i\}_{1 \leq i \leq m}$, which is not obvious. For instance, if we consider an arbitrary domain with a reentrant corner and a covering $\bigcup_{i=1}^m \Omega_i$ which is chosen in such a way that no subdomain contains an entire neighbourhood of the reentrant corner, the functions σ_i corresponding to the adjacent patches Ω_i are definitely bound to have a singularity at the reentrant corner. Unfortunately, in a practical application, such situations cannot always be avoided.

As a prototypical example, in the sequel, we analyze this problem for the special situation of the L-shaped domain being decomposed into two overlapping patches. It is shown that, despite the appearance of the mentioned singularities, all necessary properties of the partition of unity can be preserved.

3.2 Gelfand Frames on the L-shaped Domain

We shall now consider the special case that $\Omega := (-1, 1)^2 \setminus [0, 1)^2$ is the L-shaped domain in \mathbb{R}^2 , decomposed into two overlapping subdomains $\Omega = \Omega_1 \cup \Omega_2$ with $\Omega_1 := (-1, 0) \times (-1, 1)$ and $\Omega_2 := (-1, 1) \times (-1, 0)$. Due to the reentrant corner at the origin, Ω can be seen as a prototype for any non-convex polygonal domain in \mathbb{R}^2 . The particular overlapping decomposition can be exploited in the construction of Gelfand frames on Ω as follows. Let $\phi : [0, \frac{3\pi}{2}] \rightarrow \mathbb{R}_{\geq 0}$ be a smooth function with $\phi(\theta) = 1$ for $\theta \leq \frac{\pi}{2}$ and $\phi(\theta) = 0$ for $\theta \geq \pi$. Then, with $(r(x), \theta(x))$ being the polar coordinates of x with respect to the reentrant corner, the functions $\sigma_1 := \phi \circ \theta$ and $\sigma_2 := 1 - \sigma_1$ form a partition of unity subordinate to the patches Ω_i in the following sense, see also [19] for the special case $s = 1$.

Lemma 3.3. *For any $u \in H_0^s(\Omega)$, $s \in \mathbb{N}$, it is $\sigma_i u \in H_0^s(\Omega_i)$ and*

$$\|\sigma_i u\|_{H^s(\Omega_i)} \lesssim \|u\|_{H^s(\Omega)}, \quad i \in \{1, 2\}. \quad (3.10)$$

For the proof of Lemma 3.3 as well as for the arguments in Section 4, we recall the following theorem from [28].

Theorem 3.4 ([28, Theorem 1.4.4.4]). *Let Ω be a bounded open subset of \mathbb{R}^n with a Lipschitz boundary Γ , and let $\rho(x)$ denote the distance from a point x to Γ . Then, for all $u \in W_0^s(L_p(\Omega))$, $1 \leq p < \infty$, such that $s - \frac{1}{p}$ is not an integer, the following property holds*

$$\rho^{-s+|\alpha|} D^\alpha u \in L_p(\Omega) \quad (3.11)$$

for all $|\alpha| \leq s$.

The proof of this theorem given in [28] essentially relies on an application of Hardy's inequality. Moreover, what will be most important for our purposes is that it follows from the proof that

$$\|\rho^{-s+|\alpha|} D^\alpha u\|_{L_p(\Omega)} \leq C(p) \|u\|_{W^s(L_p(\Omega))}, \quad \text{for all } |\alpha| \leq s, \quad (3.12)$$

with a constant $C(p) > 0$ staying uniformly bounded as p tends to infinity.

Proof of Lemma 3.3. It suffices to treat the case $i = 1$, since the claim for $i = 2$ follows by analogy. We will show first that (3.10) holds uniformly in $u \in H_0^s(\Omega)$. To this end, for any $\alpha \in \mathbb{N}_0^n$ with $|\alpha| \leq s$, we want to use the multivariate Leibniz rule

$$D^\alpha(\sigma_1 u) = D^\alpha((\phi \circ \theta)u) = \sum_{0 \leq \beta \leq \alpha} \binom{\alpha}{\beta} D^\beta(\phi \circ \theta) D^{\alpha-\beta} u, \quad (3.13)$$

which holds as an equality in $L_2(\Omega)$ if the right-hand side is contained in $L_2(\Omega)$. Now, using Theorem 3.4 for $p = 2$, it follows that $\rho^{-s+|\alpha-\beta|} D^{\alpha-\beta} u \in L_2(\Omega)$ with

$$\|\rho^{-s+|\alpha-\beta|} D^{\alpha-\beta} u\|_{L_2(\Omega)} \lesssim \|u\|_{H^s(\Omega)} \quad (3.14)$$

for all $0 \leq \beta \leq \alpha$. It hence remains to prove that the corresponding weak derivatives of the factors $\phi \circ \theta$ in (3.13) are compensated by the additional powers of $\rho \leq r$, i.e., that

$$\|D^\beta(\phi \circ \theta) r^{s-|\alpha-\beta|}\|_{L_\infty(\Omega_1)} < \infty \quad (3.15)$$

holds for all $0 \leq \beta \leq \alpha$. In fact, (3.15) implies that

$$\|D^\beta(\phi \circ \theta) D^{\alpha-\beta} u\|_{L_2(\Omega_1)} \leq \|D^\beta(\phi \circ \theta) r^{s-|\alpha-\beta|}\|_{L_\infty(\Omega_1)} \|\rho^{-s+|\alpha-\beta|} D^{\alpha-\beta} u\|_{L_2(\Omega)} \lesssim \|u\|_{H^s(\Omega)}.$$

In the case of $\beta = 0$, (3.15) is ensured by $0 \leq \phi(\theta) \leq 1$ and the boundedness of Ω_1 . For $|\beta| \geq 1$, we utilize a multivariate Faà di Bruno formula (see Corollary 2.10 of [14]) to compute

$$D^\beta(\phi \circ \theta) = \beta! \sum_{k=1}^{|\beta|} (\phi^{(k)} \circ \theta) \sum_{(k_1, \dots, k_{|\beta|}, \nu_1, \dots, \nu_{|\beta|}) \in p(\beta, k)} \prod_{j=1}^{|\beta|} \frac{(D^{\nu_j} \theta)^{k_j}}{k_j! (\nu_j!)^{k_j}} \quad (3.16)$$

which has to be understood as a pointwise identity. Here $p(\beta, k)$ is the set of all tuples $(k_1, \dots, k_{|\beta|}, \nu_1, \dots, \nu_{|\beta|})$ with $k_j \in \mathbb{N}_0$, $\nu_j \in \mathbb{N}_0^n$, such that $\sum_{j=1}^{|\beta|} k_j = k$, $\sum_{j=1}^{|\beta|} k_j \nu_j = \beta$ and there exists some $1 \leq \ell \leq |\beta|$ with $k_j = 0$ and $\nu_j = \mathbf{0}$ for $1 \leq j \leq |\beta| - \ell$, $k_j > 0$ for $|\beta| - \ell + 1 \leq j \leq |\beta|$ and the lexicographic order $0 \prec \nu_{|\beta|-\ell+1} \prec \dots \prec \nu_{|\beta|}$.

Now a simple induction shows the existence of $h_\nu \in C^\infty[0, \frac{3}{2}\pi]$, $\nu \in \mathbb{N}_0^n$, such that

$$D^\nu \theta = (h_\nu \circ \theta) r^{-|\nu|}. \quad (3.17)$$

Using (3.16) and the boundedness of $\phi^{(k)} \circ \theta$ on Ω_1 , we get

$$\|D^\beta(\phi \circ \theta) r^{s-|\alpha-\beta|}\|_{L_\infty(\Omega_1)} \lesssim \sum_{k=1}^{|\beta|} \sum_{(k_1, \dots, k_{|\beta|}, \nu_1, \dots, \nu_{|\beta|}) \in p(\beta, k)} \left\| \prod_{j=1}^{|\beta|} (D^{\nu_j} \theta)^{k_j} r^{s-|\alpha-\beta|} \right\|_{L_\infty(\Omega_1)},$$

so that $s - |\alpha - \beta| \geq |\beta| = \sum_{m=1}^n \sum_{j=1}^{|\beta|} k_j (\nu_j)_m = \sum_{j=1}^{|\beta|} k_j |\nu_j|$ and (3.17) yield (3.15), showing that $\sigma_1 u \in H^s(\Omega_1)$ and that (3.10) holds uniformly in $u \in H_0^s(\Omega)$.

In order to see that $\sigma_1 u \in H_0^s(\Omega_1)$, let us denote with $\Gamma_{1,1}, \dots, \Gamma_{1,4}$ the open segments of $\partial\Omega_1$ and with n_l the outward normal with respect to $\Gamma_{1,l}$, $l = 1, \dots, 4$, cf. Figure 1. Moreover, with $\text{tr}_l v$ we denote the restriction of a $v \in H^s(\Omega_1)$ to $\Gamma_{1,l}$. Using this notation it is

$$H_0^s(\Omega_1) = \{v \in H^s(\Omega_1) : \text{tr}_l \frac{\partial^j v}{\partial n_l^j} = 0, \ 1 \leq l \leq 4, \ 0 \leq j \leq s-1\},$$

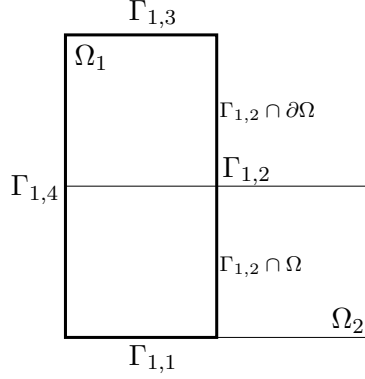


Figure 1: Decomposition of the boundary of Ω_1 into four segments.

see also [28, Theorem 1.5.2.1, Remark 1.5.2.11]. Since $u \in H_0^s(\Omega)$, we can choose test functions $u_k \in C_0^\infty(\Omega)$, $k \in \mathbb{N}$, with $u_k \rightarrow u$ in $H^s(\Omega)$. Now, as a special case, (3.13) implies that

$$\frac{\partial^j(\sigma_1 u_k)}{\partial n_l^j} = \sum_{\ell=0}^j \binom{j}{\ell} \frac{\partial^\ell(\phi \circ \theta)}{\partial n_l^\ell} \frac{\partial^{j-\ell} u_k}{\partial n_l^{j-\ell}}, \quad j = 0, \dots, s-1.$$

And a Taylor expansion at the origin yields $|D^\beta u_k| \leq C_k r^s$ for all $|\beta| \leq s$. Furthermore, using the fact that $\phi^{(k)}(\theta) = 0$, for all $k \geq 0$ and $\theta \geq \pi$ and combining (3.16) and (3.17), it becomes obvious that

$$D^\beta(\phi \circ \theta) = (\tilde{h}_\beta \circ \theta) r^{-|\beta|}, \quad \beta \in \mathbb{N}_0^n,$$

where $\tilde{h}_\beta \in C^\infty[0, \frac{3}{2}\pi]$, $\tilde{h}_\beta(\theta) = 0$, for $\theta \geq \pi$. Together with the boundedness of the restricted test functions $u_k|_{\Omega_1}$ and all its derivatives then follows

$$\text{tr}_l(\sigma_1 u_k) = \text{tr}_l \frac{\partial(\sigma_1 u_k)}{\partial n_l} = \dots = \text{tr}_l \frac{\partial^{s-1}(\sigma_1 u_k)}{\partial n_l^{s-1}} = 0, \quad l = 1, \dots, 4.$$

Thus, it is $\sigma_1 u_k \in H_0^s(\Omega_1)$ for all $k \in \mathbb{N}$. Combining this with (3.10) and the boundedness of the trace operator from $H^{s-j}(\Omega_1)$ to $H^{s-j-1/2}(\partial\Omega_1)$, $j = 0, \dots, s-1$, we finally arrive at

$$\begin{aligned} \left\| \frac{\partial^j(\sigma_1 u)}{\partial n_l} \right\|_{H^{s-j-1/2}(\partial\Omega_1)} &\leq \left\| \frac{\partial^j(\sigma_1(u - u_k))}{\partial n_l} \right\|_{H^{s-j-1/2}(\partial\Omega_1)} \lesssim \left\| \frac{\partial^j(\sigma_1(u - u_k))}{\partial n_l} \right\|_{H^{s-j}(\Omega_1)} \\ &\lesssim \|\sigma_1(u - u_k)\|_{H^s(\Omega_1)} \lesssim \|u - u_k\|_{H^s(\Omega)}, \end{aligned}$$

for $j = 0, \dots, s-1$, which tends to zero as $k \rightarrow \infty$, so that $\sigma_1 u \in H_0^s(\Omega_1)$. \square

4 Nonlinear Approximation by Aggregated Gelfand Frames

In the context of adaptive algorithms for the solution of problem (2.1) naturally arises the question which is the best convergence rate that can be obtained in terms of the relation

between the error of approximation and the number of unknowns. Typically, the benchmark for this *optimal* rate is the convergence order of a best N -term approximation of the solution u . Classical results in the context of discretizations with respect to wavelet bases yield that this benchmark depends on the Besov regularity of u in a certain scale. In this section, we analyze this coherence for the case of aggregated Gelfand frames on the L-shaped domain from Section 3.2.

It can be easily deduced from the definition, that, if Ψ is a wavelet Gelfand frame for the Gelfand triple $(H_0^s(\Omega), L_2(\Omega), H^{-s}(\Omega))$ with a dual frame $\tilde{\Psi}$, then we have the equivalence

$$\|u\|_{H^s(\Omega)} \approx \|\mathbf{u}\|_{\ell_2(\mathcal{I})}, \text{ for all } u \in H_0^s(\Omega), \quad (4.1)$$

where $\mathbf{u} = (2^{s|\lambda|}\langle u, \tilde{\psi}_\lambda \rangle_{L_2})_{\lambda \in \mathcal{I}}$. More general, if $\mathbf{c} = (c_\lambda)_{\lambda \in \mathcal{I}} \in \ell_{2,2^s}(\mathcal{I})$ is any sequence of coefficients such that $\mathbf{c}^\top \Psi = u$ with convergence in $H_0^s(\Omega)$, then one can only ensure

$$\|u\|_{H^s(\Omega)} \lesssim \|(2^{s|\lambda|}c_\lambda)_{\lambda \in \mathcal{I}}\|_{\ell_2(\mathcal{I})}, \quad (4.2)$$

because of the boundedness of $F^* : \ell_{2,2^s}(\mathcal{I}) \rightarrow H_0^s(\Omega)$, but not vice versa. However, if we intend to study the convergence rates of best N -term approximation in $H_0^s(\Omega)$, the problem can be shifted to the coefficient level. That means one may study the properties of a best N -term approximation of any sequence of expansion coefficients in $\ell_2(\mathcal{I})$. Surely, then the analysis still depends on the choice of the coefficients, and it is not a priori clear whether other choices lead to better results. In this section, we will show that for the coefficients of u with respect to the non-canonical dual frame given in (3.8), under slightly stronger assumptions on u , similar results can be obtained as in the well-known theory for the case of wavelet bases. Since it cannot be expected to obtain better rates of approximation in the case of aggregated wavelet frames, this will be the justification for our special choice of expansion coefficients for u .

In the following subsection, we briefly recall the concept of best N -Term approximation in $\ell_2(\mathcal{I})$.

4.1 N -Term Approximation

For $N = 1, 2, \dots$, let Σ_N denote the nonlinear subspace of $\ell_2(\mathcal{I})$ consisting of all vectors with at most N nonzero coordinates. Given $\mathbf{v} \in \ell_2(\mathcal{I})$, we introduce the error of approximation

$$\sigma_N(\mathbf{v}) := \inf_{\mathbf{w} \in \Sigma_N} \|\mathbf{v} - \mathbf{w}\|_{\ell_2(\mathcal{I})}. \quad (4.3)$$

Clearly, a best approximation to \mathbf{v} from Σ_N is obtained by taking a vector $\mathbf{v}_N \in \Sigma_N$, which agrees with \mathbf{v} on those coordinates on which \mathbf{v} takes its N largest values in modulus, and which is zero everywhere else. Thus, \mathbf{v}_N is called a best N -term approximation to \mathbf{v} . Note that it is not necessarily unique.

The concept of best N -term approximation is closely related to the *weak* ℓ_τ -spaces $\ell_\tau^w(\mathcal{I})$. Given some $0 < \tau < 2$, $\ell_\tau^w(\mathcal{I})$ is defined as

$$\ell_\tau^w(\mathcal{I}) := \{\mathbf{c} \in \ell_2(\mathcal{I}) : |\mathbf{c}|_{\ell_\tau^w} := \sup_{k \in \mathbb{N}} k^{1/\tau} |\gamma_k(\mathbf{c})| < \infty\}, \quad (4.4)$$

where $\gamma_k(\mathbf{c})$ is the k th largest coefficient in modulus of \mathbf{c} . Then, for each $s > 0$,

$$\sup_N N^s \sigma_N(\mathbf{v}) \approx |\mathbf{v}|_{\ell_\tau^w}, \quad (4.5)$$

where s and τ are related according to

$$\tau = \left(s + \frac{1}{2} \right)^{-1}.$$

Hence $\mathbf{v} \in \ell_\tau^w(\mathcal{I})$, if and only if the error of a best N -term approximation is of the order $\mathcal{O}(N^{-s})$. Note that $\ell_\tau(\mathcal{I}) \hookrightarrow \ell_\tau^w(\mathcal{I}) \hookrightarrow \ell_{\tau+\gamma}(\mathcal{I})$, for a $\gamma \in (0, 2 - \tau]$. The expression $|\mathbf{v}|_{\ell_\tau^w}$ defines only a quasi-norm since it does not necessarily satisfy the triangle inequality. Yet, for each $0 < \tau < 2$, there exists a $C(\tau) > 0$ with

$$|\mathbf{v} + \mathbf{w}|_{\ell_\tau^w} \leq C(\tau) (|\mathbf{v}|_{\ell_\tau^w} + |\mathbf{w}|_{\ell_\tau^w}), \quad \mathbf{v}, \mathbf{w} \in \ell_\tau^w(\mathcal{I}). \quad (4.6)$$

We refer to [10, 27] for further details on the quasi-Banach spaces $\ell_\tau^w(\mathcal{I})$.

A classical result from the theory of nonlinear approximation with wavelet Riesz bases reads as follows. Let $(\Psi, \tilde{\Psi})$ be a pair of biorthogonal wavelet Riesz bases for $L_2(\Omega)$ such that Ψ gives rise for a characterization of the Sobolev space $H_0^t(\Omega)$, cf. (2.16), say for a $t > 0$. Hence, with $D = \text{diag}(2^{|\lambda|t})_{\lambda \in \mathcal{I}}$, $D^{-1}\Psi$ is actually a Riesz basis for $H_0^t(\Omega)$. Further, let Ψ be of order d , meaning that locally polynomials up to degree $d - 1$ can be represented. Then, it is well-known (see [9]) that for sufficiently smooth wavelets, and $0 < s < (d - t)/n$, one has the relation

$$u \in B_\tau^{sn+t}(L_\tau(\Omega)) \quad \text{if and only if} \quad D\tilde{F}u = \left(2^{|\lambda|t} \langle u, \tilde{\psi}_\lambda \rangle_{L_2(\Omega)} \right)_{\lambda \in \mathcal{I}} \in \ell_\tau(\mathcal{I}), \quad (4.7)$$

where $\tau = (s + \frac{1}{2})^{-1}$, and $D\tilde{F}u$ are exactly the unique expansion coefficients of u with respect to the Riesz basis $D^{-1}\Psi$ in $H_0^t(\Omega)$. Here, as usual, $B_\tau^\alpha(L_\tau(\Omega))$ denotes the classical Besov space measuring smoothness up to order α in $L_\tau(\Omega)$. Consequently, since $\ell_\tau(\mathcal{I}) \hookrightarrow \ell_\tau^w(\mathcal{I})$, if $u \in B_\tau^{sn+t}(L_\tau(\Omega))$, then the error of its best N -term approximation with respect to $\|\cdot\|_{H^t}$ decays like N^{-s} . In the next subsection, we want to prove that the latter statement can be carried over to case of aggregated wavelet frames on the L-shaped domain by applying (4.7) separately on each patch Ω_i .

4.2 The L-shaped Domain

In the sequel, our analysis will be restricted to the case of elliptic operator equations

$$\mathcal{L}u = f \quad (4.8)$$

of integer order $2t$, $t \geq 1$, where $\mathcal{L} : H_0^t(\Omega) \rightarrow H^{-t}(\Omega)$, on the L-shaped domain Ω from Section 3.2, i.e., $n = 2$. We will consider a Gelfand frame $\Psi = \Psi^{(1)} \cup \Psi^{(2)}$ for $H_0^t(\Omega)$, where the local bases $\Psi^{(i)}$ are chosen to be biorthogonal wavelet Riesz bases of approximation order $d \geq t + 1$ such that (4.7) holds for the pair $(\Psi^{(i)}, \tilde{\Psi}^{(i)})$ in Ω_i . A sufficient smoothness of the wavelets will be tacitly assumed.

According to the remarks at the beginning of Section 4, first of all one has to choose a representation of u with respect to Ψ . Proposition 3.2 implies that an arbitrary $u \in H_0^t(\Omega)$ can be represented according to

$$u = \sum_{i=1}^2 \sum_{\lambda \in \mathcal{I}^\square} \langle u, \sigma_i \tilde{\psi}_{i,\lambda} \rangle_{L_2} \psi_{i,\lambda} = \sum_{i=1}^2 \sum_{\lambda \in \mathcal{I}^\square} 2^{t|\lambda|} \langle u, \sigma_i \tilde{\psi}_{i,\lambda} \rangle_{L_2} 2^{-t|\lambda|} \psi_{i,\lambda},$$

with convergence of the series in $H_0^t(\Omega)$, where $\{\sigma_i\}_{i=1,2}$ is the partition of unity given at the beginning of Section 3.2. Throughout the rest of this section, the properties of a best N -term approximation of the sequence of expansion coefficients

$$\mathbf{u} = (2^{t|\lambda|} \langle u, \sigma_i \tilde{\psi}_{i,\lambda} \rangle)_{\lambda \in \mathcal{I}^\square, i=1,2} \quad (4.9)$$

shall be analyzed. Obviously, in order to be able to use (4.7), it will be necessary to develop a Besov regularity analysis of the products $\sigma_i u$. To this end, it will turn out to be beneficial to make the following assumption on the solution u of (4.8). Therein and throughout the present section we denote with $(r(x, y), \theta(x, y))$ polar coordinates with respect to the reentrant corner.

Assumption 4.1. (i) Let the solution u to (4.8) be contained in $H^{t+\nu}(\Omega)$, for a $\nu > 0$.

(ii) Let for all multi-indices α with $|\alpha| = j$, $j = 0, \dots, t$, the solution u to (4.8) satisfy

$$D^\alpha u(x, y) = \mathcal{O}(r(x, y)^{\beta_j}), \text{ for } r(x, y) \rightarrow 0, \text{ with } \beta_j > t - (j + 1). \quad (4.10)$$

In Subsections 4.2.1 and 4.2.2 below, it will be carried out that for the Poisson and the biharmonic equation on the L-shaped domain these assumptions are actually satisfied, provided that the right-hand side f fulfills a rather mild requirement on its Sobolev regularity.

Note that if u satisfies part (ii) of the assumption, then without loss of generality we may also assume $t - j > \beta_j$. In fact, if a function is of the order r^β , for $r \rightarrow 0$, then it is surely also of the order $r^{\tilde{\beta}}$ for all $\tilde{\beta} < \beta$. We will make use of this observation in the proof of the next proposition, where we want to establish Sobolev regularity for $u_1 = \sigma_1 u = (\phi \circ \theta)u$ and $u_2 = (1 - \sigma_1)u$.

Proposition 4.2. *Let Assumption 4.1 be satisfied. Then, there exists a sufficiently small $\eta > 0$ such that u_1 and u_2 are contained in $H^{t+\eta}(\Omega)$.*

For the proofs of Proposition 4.2 and Lemma 4.7, we shall need the following Besov function multiplier theorem [36, Theorem 2, Section 4.4.4] and a simple conclusion thereof.

Theorem 4.3. *Suppose that the following conditions are valid:*

- (i) $0 < s_1 < s_2$,
- (ii) $\frac{1}{p} \leq \frac{1}{p_1} + \frac{1}{p_2}$,
- (iii) $\frac{2}{p} - s_1 = (\frac{2}{p_1} - s_1)_+ + (\frac{2}{p_2} - s_2)_+$ and $\max_i (\frac{2}{p_i} - s_i)_+ > 0$,

$$(iv) \quad s_1 + s_2 > \frac{2}{p_1} + \frac{2}{p_2} - 2,$$

$$(v) \quad q \geq q_1,$$

$$(vi) \quad q \geq q_2 \quad \text{if} \quad s_1 - \frac{2}{p} = s_2 - \frac{2}{p_2},$$

$$(vii) \quad \{i \in \{1, 2\} : s_i = \frac{2}{p_i} \text{ and } q_i > 1\} \cup \{i \in \{1, 2\} : s_i < \frac{2}{p_i} \text{ and } q_i > \frac{2}{\frac{2}{p_i} - s_i}\} = \emptyset.$$

Then we have the continuous embedding $B_{q_1}^{s_1}(L_{p_1}(\Omega)) \cdot B_{q_2}^{s_2}(L_{p_2}(\Omega)) \hookrightarrow B_q^{s_1}(L_p(\Omega))$.

Corollary 4.4. *Assume that $f \in H^\nu(\Omega)$ for some $0 < \nu < 1$ and that $g \in H^\eta(\Omega)$ for all $\nu < \eta < 1$. Then fg is contained in $H^{\nu-\varepsilon}(\Omega)$ for all $\varepsilon > 0$.*

Proof. It is sufficient to prove that $fg \in B_2^\nu(L_p(\Omega))$ for all $\frac{2}{2-\nu} < p < 2$, since for any sufficiently small $\varepsilon > 0$ we can pick $p = \frac{4}{2+\varepsilon} < 2$ and append the continuous embeddings

$$B_2^\nu(L_p(\Omega)) \hookrightarrow B_p^{\nu-\varepsilon/2}(L_p(\Omega)) \hookrightarrow H^{\nu-\varepsilon/2-2(1/p-1/2)}(\Omega) = H^{\nu-\varepsilon}(\Omega).$$

For any $\frac{2}{2-\nu} < p < 2$, setting $s_2 = 2 - \frac{2}{p}$, we have $\nu < s_2 < 1$ and hence $g \in H^\eta(\Omega) \hookrightarrow H^{s_2}(\Omega)$ for all $s_2 < \eta < 1$. We shall apply Theorem 4.3 for $p_1 = p_2 = q_1 = q_2 = q = 2$ and $s_1 = \nu$ to finish the proof. In fact, by $s_2 > \nu = s_1$, condition (i) is satisfied. Using $p > \frac{2}{2-\nu} > 1$, we have $\frac{1}{p} < 1 = \frac{1}{p_1} + \frac{1}{p_2}$ and hence condition (ii) holds. Since $\nu < 1$, it is $\frac{2}{p_1} - s_1 = 1 - \nu > 0$, so that condition (iii) can be verified by

$$\left(\frac{2}{p_1} - s_1\right)_+ + \left(\frac{2}{p_2} - s_2\right)_+ - \left(\frac{2}{p} - s_1\right) = 2 - s_2 - \frac{2}{p} = 0.$$

Condition (iv) holds due to $s_1 + s_2 = \nu + s_2 > 0 = \frac{2}{p_1} + \frac{2}{p_2} - 2$, and condition (v) is true by the choice $q = q_1 = 2$. Since $s_1 - \frac{2}{p} - (s_2 - \frac{2}{p_2}) = \nu - 1 < 0$, there is nothing to prove for condition (vi). Finally, the first set in condition (vii) is empty by $p_i = 2$ and $s_i < 1$, and the second set is empty due to $\frac{2}{\frac{2}{p_1} - s_1} = \frac{2}{1-\nu} > 2 = q_1$ and $\frac{2}{\frac{2}{p_2} - s_2} = \frac{2}{\frac{2}{p} - 1} > \frac{2}{1-\nu} > 2 = q_2$. \square

Proof of Proposition 4.2. It is sufficient to show that $u_1 \in H^{t+\eta}(\Omega)$ for some $\eta > 0$, since then the statement for u_2 follows from $u_2 = (1 - \sigma_1)u$. Given any $\alpha \in \mathbb{N}_0^n$ with $|\alpha| = t$, it will be our strategy to verify that $D^\alpha u_1 \in H^\eta(\Omega)$ by showing that $D^\alpha u_1 \in W^1(L_p(\Omega))$ for some $p > 1$, since then the claim follows by the Sobolev embedding theorem. By the representation (3.13), we can decompose $D^\alpha u_1$ into

$$D^\alpha u_1 = (\phi \circ \theta)D^\alpha u + \sum_{\substack{0 \leq \beta \leq \alpha \\ \beta \neq 0}} \binom{\alpha}{\beta} D^\beta(\phi \circ \theta)D^{\alpha-\beta}u. \quad (4.11)$$

We shall treat both addends in (4.11) separately. For the first one, note that $D^\alpha u \in H^\nu(\Omega)$ by Assumption 4.1 (i). Moreover, using (3.17), we clearly have

$$\left\| \frac{\partial(\phi \circ \theta)}{\partial x_j} \right\|_{L_p(\Omega)}^p = \int_{\Omega} |h_{e_j} \circ \theta|^p r^{-p} dx_1 dx_2 \lesssim \int_0^{\sqrt{2}} r^{1-p} dr$$

which is finite for all $1 \leq p < 2$. Hence, by the Sobolev embedding theorem, it is $\phi \circ \theta \in H^\eta(\Omega_1)$ for all $0 < \eta < 1$, so that Corollary 4.4 implies $(\phi \circ \theta)D^\alpha u \in H^\eta(\Omega)$ for all $0 < \eta < \nu$.

It remains to study the rightmost sum in (4.11). For one single addend, (3.17) and Assumption 4.1 (ii) imply that

$$\begin{aligned} \left\| \frac{\partial D^\beta(\phi \circ \theta)D^{\alpha-\beta}u}{\partial x_j} \right\|_{L_p(\Omega)}^p &\lesssim \int_{\Omega} |(h_{\beta+e_j} \circ \theta)D^{\alpha-\beta}u|^p r^{-(|\beta|+1)p} dx_1 dx_2 \\ &\quad + \int_{\Omega} |(h_{\beta} \circ \theta)D^{\alpha+e_j-\beta}u|^p r^{-|\beta|p} dx_1 dx_2 \\ &\lesssim \int_0^{\sqrt{2}} (r^{\beta_{|\alpha-\beta|-|\beta|-1}} + r^{\beta_{|\alpha+e_j-\beta|-|\beta|}})^p r dr \\ &\lesssim \int_0^{\sqrt{2}} r^{p \min\{\beta_{|\alpha-\beta|-|\beta|-1}, \beta_{|\alpha+e_j-\beta|-|\beta|}\}+1} dr < \infty, \end{aligned}$$

if $p \min\{\beta_{|\alpha-\beta|-|\beta|-1}, \beta_{|\alpha+e_j-\beta|-|\beta|}\} > -2$. Since $\beta_{|\gamma|} < t - |\gamma|$ for all $\gamma \in \mathbb{N}_0^n$ with $|\gamma| \leq t$, the sufficient condition on p is equivalent to

$$p < \frac{2}{\max\{|\beta| + 1 - \beta_{|\alpha-\beta|}, |\beta| - \beta_{|\alpha+e_j-\beta|}\}} < 2. \quad (4.12)$$

Because of Assumption 4.1 (ii), $\frac{2}{\max\{|\beta|+1-\beta_{|\alpha-\beta|}, |\beta|-\beta_{|\alpha+e_j-\beta|}\}} > 1$. Consequently, there exists a $\tilde{p} \in (1, 2)$, such that the rightmost sum in (4.11) is contained in $W^1(L_{\tilde{p}}(\Omega))$, for all $1 \leq p \leq \tilde{p}$, and a simple application of the Sobolev embedding theorem gives the existence of an $\eta > 0$ such that it is contained in $H^\eta(\Omega)$. \square

By now, we have utilized several times that the α -th derivative of $\sigma_1 = \phi \circ \theta$ introduces a factor $r^{-|\alpha|}$. In order to ensure specific properties of a product $\sigma_1 u$, additional assumptions on the cofactor u are then needed to compensate these singularities near the reentrant corner. Lemma 3.3 showed that appropriate boundary conditions, $u \in H_0^t(\Omega)$, are sufficient to guarantee that $\sigma_1 u \in H_0^t(\Omega_1)$. In order to obtain higher order Sobolev regularity of $\sigma_1 u$, Proposition 4.2 reveals that Assumption 4.1 (ii) is the adequate one.

We are now in a position to formulate the main result of this section, stating that the frame coefficients (4.9) of the solution u exhibit a certain decay, i.e., they must be contained in $\ell_\tau(\mathcal{I})$, for a certain range of $0 < \tau < 2$.

Theorem 4.5. *Let u be the solution to (4.8), and let Assumption 4.1 be satisfied. For $s > t$ and $\delta \in (0, s-t)$, let $u \in B_\tau^s(L_\tau(\Omega))$, where $\frac{1}{\tau} = \frac{s-(t+\delta)}{2} + \frac{1}{2}$. Then, there exists a sufficiently small $\eta > 0$ such that the sequence of frame coefficients $(2^{t|\lambda|} \langle u, \sigma_i \tilde{\psi}_{i,\lambda} \rangle)_{\lambda \in \mathcal{I}^\square, i=1,2}$ belongs to the space $\ell_{\tau_0}(\mathcal{I})$, where $\frac{1}{\tau_0} = \frac{s'-t}{2} + \frac{1}{2}$, for all $t < s' < \min\{d, \frac{\eta s+t-1}{t+\eta-1} + t-1\} =: s^*$.*

Here we have assumed that u is contained in a scale of Besov spaces which lies slightly above the classical scale of spaces which govern the convergence rates for best N -term approximation in $H^t(\Omega)$, see the DeVore/Triebel-diagram in Figure 2. At the end of Section 4.2 we will show that, under mild regularity assumptions on the right-hand side f , also this requirement is satisfied for the weak solutions of the Poisson and the biharmonic equation with homogeneous Dirichlet boundary conditions.

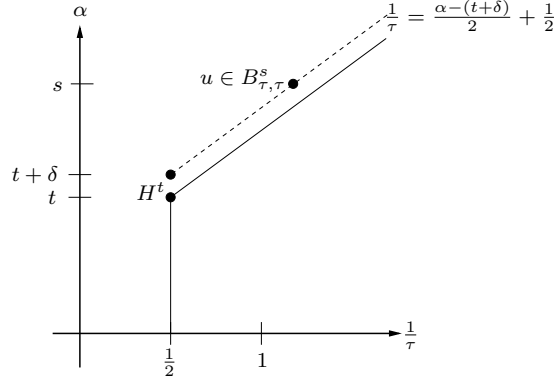


Figure 2: Classical scale of Besov spaces governing best N -term approximation in $H^t(\Omega)$ w.r.t. wavelet bases (solid line), and the relevant scale for the case of aggregated wavelet frames (dashed line).

The proof of Theorem 4.5 will be based on well-known embedding theorems for Sobolev spaces and on interpolation arguments between Sobolev and Besov spaces, see [1, 27]. In particular, the principal idea is to show that u_i is contained in $B_\tau^{s'}(L_\tau(\Omega_i))$, $\frac{1}{\tau} = \frac{s'-t}{2} + \frac{1}{2}$, for all $t < s' < s^*$ and then to employ (4.7) with respect to the local biorthogonal pairs of wavelet bases $(\Psi^{(i)}, \tilde{\Psi}^{(i)})$, $i = 1, 2$.

As an initial step, we want to establish Besov regularity for u_1 and u_2 . We start with the factor σ_1 .

Lemma 4.6. *For any $s \geq 1 - \varepsilon$, the function $\sigma_1 = \phi \circ \theta$ is contained in $B_\tau^s(L_\tau(\Omega))$, for $\frac{1}{\tau} = \frac{s-(1-\varepsilon)}{2} + \frac{1}{2}$, where ε may be chosen arbitrarily small.*

Proof. As we have seen in the proof of Proposition 4.2, $\sigma_1 = \phi \circ \theta \in H^\alpha(\Omega)$ for all $\alpha \in (0, 1)$. Furthermore, analogous to the proof of [15, Theorem 2.3], one can show that $\sigma_1 \in B_\tau^{s'}(L_\tau(\Omega))$, $\frac{1}{\tau} = \frac{s'}{2} + \frac{1}{2}$ for any $s' > 0$. The asserted statement then immediately follows by employing real interpolation between the latter Besov spaces and $H^\alpha(\Omega)$, $\alpha \in (0, 1)$. \square

Using Lemma 4.6 and Theorem 4.3, we obtain

Lemma 4.7. *Let $s > t$. If u is contained in $B_\tau^s(L_\tau(\Omega))$, for a $\delta \in (0, s - t)$ and $\frac{1}{\tau} = \frac{s-(t+\delta)}{2} + \frac{1}{2}$, then $u_1 = \sigma_1 u \in B_{\tau'}^{s'}(L_{\tau'}(\Omega))$, $\frac{1}{\tau'} = \frac{s'-(1-\varepsilon)}{2} + \frac{1}{2}$ for any $s' \in [1 - \varepsilon, s)$ and for any $\varepsilon \in (0, 2 + \delta)$.*

Proof. Lemma 4.6 tells us that $\sigma_1 \in B_{\tau'}^{s'}(L_{\tau'}(\Omega))$, $\frac{1}{\tau'} = \frac{s'-(1-\varepsilon)}{2} + \frac{1}{2}$ for any $s' > 0$. It is therefore sufficient to verify that $B_{\tau'}^{s'}(L_{\tau'}(\Omega)) \cdot B_\tau^s(L_\tau(\Omega)) \hookrightarrow B_{\tau'}^{s'}(L_{\tau'}(\Omega))$, for $s > s'$, by an application of Theorem 4.3. To this end, let us denote $s_2 = s$, $s_1 = s'$, $p_1 = q_1 = p = q = \tau'$ and $p_2 = q_2 = \tau$. Since $s > s' > 0$, condition (i) holds, and the validity of condition (ii) follows from $p = p_1$ and $p_2 > 0$. We clearly have $\frac{2}{p_1} - s_1 = \frac{2}{\tau'} - s' = \varepsilon > 0$, so that condition (iii) is verified by $\frac{2}{p_2} - s_2 = -\delta - t + 1 < 0$. Furthermore, we have $s_1 + s_2 = \frac{2}{p_1} + \frac{2}{p_2} - \varepsilon + \delta + t - 1 > \frac{2}{p_1} + \frac{2}{p_2} - 2$, for any $0 < \varepsilon < \delta + 2$, and since $\frac{2}{p_2} - s_2 = -\delta - t + 1 \neq \varepsilon = \frac{2}{p_1} - s_1$ both conditions (iv) and (vi) are satisfied. For condition (v), there is nothing to prove due to $q = q_1 = \tau'$. Moreover, the set $\{i \in \{1, 2\} : s_i = \frac{2}{p_i} \text{ and } p_i > 1\}$ is clearly empty. We

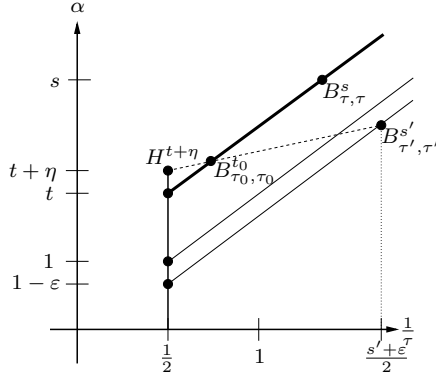


Figure 3: DeVore-Triebel diagram corresponding to the proof of Theorem 4.5.

have $s_2 > \frac{2}{\tau_2}$ and $\frac{2}{s_1 + \varepsilon} = p_1 < \frac{2}{\frac{2}{p_1} - s_1} = \frac{2}{\varepsilon}$, for $\varepsilon > 0$ arbitrarily small, ensuring the validity of condition (vii). Therefore, we can apply Theorem 4.3 and conclude the proof. \square

Finally, we are now prepared to prove our main result of this section.

Proof of Theorem 4.5. Lemma 4.7 implies $u_i = \sigma_i u \in B_{\tau'}^{s'}(L_{\tau'}(\Omega))$, $\frac{1}{\tau'} = \frac{s' - (1 - \varepsilon)}{2} + \frac{1}{2}$ for any $s' \in [1 - \varepsilon, s)$ and for any $\varepsilon \in (0, 2 + \delta)$. Moreover, Proposition 4.2 gives $u_i \in H^{t + \eta}(\Omega)$, for an $\eta > 0$, and by using real interpolation between $H^{t + \eta}(\Omega)$ and $B_{\tau'}^{s'}(L_{\tau'}(\Omega))$, it can be easily checked that $u_i \in B_{\tau_0}^{t_0}(L_{\tau_0}(\Omega))$, where $\frac{1}{\tau_0} = \frac{t_0 - t}{2} + \frac{1}{2}$ and $t_0 = (t + \eta + \varepsilon - 1)^{-1}((\eta + 1)(s' + \varepsilon - 1) - (s' - t - \eta)) + t - 1$. Indeed, t_0 is obtained by computing the intersection of the bold-faced and the dashed line in the DeVore-Triebel diagram in Figure 3. For $\varepsilon \rightarrow 0$ and $s' \rightarrow s$, t_0 tends to $\frac{\eta s + t - 1}{t + \eta - 1} + t - 1$. Consequently, since ε may be chosen arbitrarily small, and since s' may be chosen arbitrarily close to s , it follows that $u_i \in B_{\check{\tau}}^{\check{s}}(L_{\check{\tau}}(\Omega))$, where $\frac{1}{\check{\tau}} = \frac{\check{s} - t}{2} + \frac{1}{2}$, for all $t < \check{s} < \frac{\eta s + t - 1}{t + \eta - 1} + t - 1$.

Finally, from Lemma 3.3 and the fact that the local systems $\Psi^{(i)}$ are Riesz bases of order d with dual bases $\tilde{\Psi}^{(i)}$, it can be inferred from (4.7) that the sequence of wavelet coefficients $(2^{t|\lambda|} \langle u, \sigma_i \tilde{\psi}_{i,\lambda} \rangle)_{\lambda \in \mathcal{I}^\square, i=1,2}$ belongs to the space $\ell_{\check{\tau}}(\mathcal{I})$ for $\frac{1}{\check{\tau}} = \frac{\check{s} - t}{2} + \frac{1}{2}$ for all $t < \check{s} < \min\{d, \frac{\eta s + t - 1}{t + \eta - 1} + t - 1\}$. \square

Throughout the rest of this section, it will be pointed out that for two prominent examples of elliptic problems, i.e., the Poisson and the biharmonic equation, Assumption 4.1 as well as the assumed Besov regularity are indeed satisfied, so that Theorem 4.5 is applicable.

4.2.1 The Poisson Equation

Let us first consider the Poisson equation with homogeneous boundary conditions on the L-shaped domain, $t = 1$. First of all, we state the following well-known theorem from [29, Chapter 2.7] which characterizes the weak solution to problem (2.5) on an arbitrary polygonal domain.

Theorem 4.8. *Let $\Omega \subset \mathbb{R}^2$ be a polygonal domain with vertices S_l , $l = 1 \dots, M$. Let the measures of the inner angles at S_l be denoted with ω_l . With respect to polar coordinates*

(r_l, θ_l) in the vicinity of each vertex S_l we introduce the functions

$$\mathcal{S}_{l,m}(r_l, \theta_l) = \zeta_l(r_l) r_l^{\lambda_{l,m}} \sin(m\pi\theta_l/\omega_l), \text{ when } \lambda_{l,m} = m\pi/\omega_l \text{ is not an integer, (4.13)}$$

$$\mathcal{S}_{l,m}(r_l, \theta_l) = \zeta_l(r_l) r_l^{\lambda_{l,m}} [\log r_l \sin(m\pi\theta_l/\omega_l) + \theta_l \cos(m\pi\theta_l/\omega_l)] \text{ otherwise. (4.14)}$$

Here ζ_l denotes a suitable C^∞ truncation function, and $m \geq 1$ is an integer. Then, for a given $f \in H^s(\Omega)$, $s \geq -1$, the corresponding variational solution to (2.5) has an expansion $u = u_R + u_S$, where $u_R \in H^{s+2}(\Omega)$ and

$$u_S = \sum_{l=1}^M \sum_{0 < \lambda_{l,m} < s+1} c_{l,m} \mathcal{S}_{l,m}, \quad (4.15)$$

provided that no $\lambda_{l,m}$ is equal to $s+1$.

Usually u_S and u_R are called *singular* and *regular part* of the solution, respectively. For the special case of the L-shaped domain, at the reentrant corner the measure of the inner angle is $\frac{3}{2}\pi$, while at all other vertices we have $\omega_l = \frac{\pi}{2}$. Using [29, Theorem 1.2.18], it can be easily inferred that in this case u_S is contained in $H^\alpha(\Omega)$, for any $\alpha < 5/3$. Therefore, with $f \in H^\mu(\Omega)$ for a $\mu > -1$, Assumption 4.1 (i) is surely satisfied. For the verification of the second part of the assumption, we state the following lemma.

Lemma 4.9. *Let u be the variational solution to (2.5) with a right-hand side $f \in H^\mu(\Omega)$ for some $\mu > 0$. Then, we have $u_R(x, y) = \mathcal{O}(r(x, y))$, and $\nabla u_R(x, y) = \mathcal{O}(1)$, for $r \rightarrow 0$. Moreover, the singular part satisfies $u_S(x, y) = \mathcal{O}(r(x, y)^{2/3})$, as well as $\nabla u_S(x, y) = \mathcal{O}(r(x, y)^{-1/3})$, for $r \rightarrow 0$.*

Proof. The statements on u_S immediately follow from Theorem 4.8. In order to prove the statements for the regular part u_R , it will be convenient to show that $u_R \in W_0^1(L_p(\Omega))$ for all $2 \leq p < \infty$. Indeed, since $u_R \in H^{2+\mu}(\Omega)$, the Sobolev embedding theorem implies $u_R \in W^1(L_p(\Omega))$, for all $2 \leq p < \infty$. Furthermore, using $u_R \in H_0^1(\Omega)$ and taking the trace in the H -scale, i.e. for $p = 2$, we get $\|\text{tr } u_R\|_{H^{\frac{1}{2}}} = 0$. Since $u_R \in H^{2+\mu}(\Omega)$, and thus for sure $u_R \in C^0(\Omega)$, any trace operator applied to u_R , i.e. for arbitrary $2 \leq p < \infty$, gives the the same result, namely $\text{tr } u_R = 0$. Hence, $u_R \in W_0^1(L_p(\Omega))$, for all $2 \leq p < \infty$.

Now Theorem 3.4 tells us that $\rho^{-1+|\alpha|} D^\alpha u_R \in L_p(\Omega)$ for all $|\alpha| \leq 1$, and in addition also

$$\|\rho^{-1+|\alpha|} D^\alpha u_R\|_{L_p(\Omega)} \lesssim \|u_R\|_{W^1(L_p(\Omega))}, \text{ for all } |\alpha| \leq 1, \quad (4.16)$$

and all $2 \leq p < \infty$, with a constant depending on p only for small p . Therefore the task is to prove that the right-hand side in (4.16) can be uniformly bounded as p approaches infinity, because in that case it clearly follows that $\rho^{-1+|\alpha|} D^\alpha u \in L_\infty(\Omega)$, $|\alpha| \leq 1$. Together with $r^{-1} \leq \rho^{-1}$, this yields $u_R(x, y) = \mathcal{O}(r(x, y))$ and $\nabla u_R(x, y) = \mathcal{O}(1)$, and thus the proof is completed.

To this end, we will again make use of the fact that $u_R \in H^{2+\varepsilon}(\Omega)$, for $0 < \varepsilon \leq \mu$. Without loss of generality we may assume $\varepsilon < 1$. Note that by the continuity of the embeddings $H^{2+\varepsilon}(\Omega) = B_2^{2+\varepsilon}(L_2(\Omega)) \hookrightarrow B_\infty^{1+\varepsilon}(L_\infty(\Omega)) \hookrightarrow C^1(\Omega)$, we may infer $u_R \in$

$C^1(\Omega)$, so that the boundedness of the first order derivative of u_R is anyway guaranteed. Hence,

$$\begin{aligned} \|u_R\|_{W^1(L_p(\Omega))} &\leq 2^{1/p} \left(\|u_R\|_{L_p(\Omega)} + \left\| \frac{\partial u_R}{\partial x} \right\|_{L_p(\Omega)} + \left\| \frac{\partial u_R}{\partial y} \right\|_{L_p(\Omega)} \right) \\ &\leq (2|\Omega|)^{1/p} \left(\|u_R\|_{L_\infty(\Omega)} + \left\| \frac{\partial u_R}{\partial x} \right\|_{L_\infty(\Omega)} + \left\| \frac{\partial u_R}{\partial y} \right\|_{L_\infty(\Omega)} \right), \end{aligned}$$

where the upper bound stays bounded as p tends to infinity. \square

Moreover, [15, Theorem 2.4] implies that the variational solution u to (2.5) is contained in $B_\tau^\alpha(L_\tau(\Omega))$, for all $\frac{3}{2} < \alpha < \mu + 2$, $\frac{1}{\tau} = \frac{\alpha - 3/2}{2} + \frac{1}{2}$, if $f \in H^\mu(\Omega)$, for $\mu > -1/2$. Therefore, the assumption in Theorem 4.5 is fulfilled by the choice $\delta = 1/2$ and $s < \mu + 2$.

Hence, we arrive at the following special result, which is a direct consequence of the latter observations and Theorem 4.5 for $t = 1$.

Corollary 4.10. *Let u be the variational solution to (2.5). Let the right-hand side f be contained in $H^\mu(\Omega)$ for a $\mu > 0$. Then, the sequence of frame coefficients $(2^{|\lambda|} \langle u, \sigma_i \tilde{\psi}_{i,\lambda} \rangle)_{\lambda \in \mathcal{I}^\square, i=1,2}$ belongs to the space $\ell_{\tau_0}(\mathcal{I})$, where $\frac{1}{\tau_0} = \frac{s-1}{2} + \frac{1}{2}$, for all $1 < s < \min\{d, \mu + 2\}$.*

It is important to stress the fact that in the case of a wavelet basis with similar regularity and approximation properties, for the unique expansion coefficients, the analogous statement holds under the only slightly milder requirement $f \in H^\mu(\Omega)$, $\mu > -1/2$.

Example 4.11. Consider the case $u = u_S$, u_S as in (4.15), and $f = -\Delta u_S$. In [15] it has been shown that for any $\alpha > 0$ each function $\mathcal{S}_{l,m}$, and thus also u_S is contained in $B_\tau^\alpha(L_\tau(\Omega))$, $\frac{1}{\tau} = \frac{\alpha}{2} + \frac{1}{2}$. Together with the fact that $u_S \in H^\omega(\Omega)$, with $\omega < 5/3$, this implies that in this case the assumption of Theorem 4.5 is satisfied for any $s > 1$. Moreover, the right-hand side f vanishes in a vicinity of the reentrant corner and is contained in $C^\infty(\bar{\Omega})$. Consequently, the sequence of frame coefficients $(2^{|\lambda|} \langle u, \sigma_i \tilde{\psi}_{i,\lambda} \rangle)_{\lambda \in \mathcal{I}^\square, i=1,2}$ belongs to $\ell_\tau(\mathcal{I})$, and thus to $\ell_\tau^w(\mathcal{I})$, for $\frac{1}{\tau} = \frac{\gamma-1}{2} + \frac{1}{2}$ and for all $1 < \gamma < d$. This means that the convergence order of the best N -term approximation is $\mathcal{O}(N^{-(\gamma-1)/2})$, for any $1 < \gamma < d$, so that in principle the order of convergence is only limited by the order d of the wavelets.

4.2.2 The Biharmonic Equation

As another important application of Theorem 4.5 we study the biharmonic problem, $t = 2$,

$$\begin{aligned} \Delta^2 u &= f \text{ in } \Omega, \\ u = \frac{\partial u}{\partial n_l} &= 0 \text{ on } \Gamma_l, \quad l = 1, \dots, 6, \end{aligned} \tag{4.17}$$

where the Γ_l denote the open segments of $\partial\Omega$ and clearly n_l the outward normal at Γ_l . We denote with S_l , $l = 1, \dots, 6$, the vertices of the L-shaped domain and declare S_1 to be the reentrant corner. Then, the inner angle ω_l at a vertex S_l is equal to $\frac{\pi}{2}$, except for S_1 , where it is $\omega_1 = \frac{3}{2}\pi$. The counterpart of Theorem 4.8 for the biharmonic equation reads as follows, cf. [29, Theorem 3.4.4].

Theorem 4.12. *Let $u \in H_0^2(\Omega)$ be the solution of (4.17) with f given in $L_2(\Omega)$. Then, there exists a function $u_R \in H^4(\Omega)$ and constants c_l , $l = 0, \dots, 6$, such that u can be written as $u = u_R + u_S$ with*

$$u_S = \eta(r)(c_0 r^{1+z_0} v(z_0, \theta) + c_1 r^{1+z_1} v(z_1, \theta)) + \sum_{l=2}^6 c_l \eta_l(r_l) r_l^2 v(1, \theta_l), \quad (4.18)$$

where $z_0 \approx 0.5445$, $z_1 \approx 0.9085$ and with $v(z, \cdot)$ being a smooth function for each fixed z . Moreover, (r_l, θ_l) denote polar coordinates with respect to the corners S_l , $l = 2, \dots, 6$, whereas η and η_l are suitable smooth cut-off functions.

For an explicit expression for $v(z, \cdot)$, the reader is referred to [29]. Another application of [29, Theorem 1.2.18] shows that u_S is at least contained in $H^{2+\varepsilon}(\Omega)$ for an $\varepsilon > 0.5$, so that Assumption 4.1 (i) is satisfied for u_S and also for u_R provided that $f \in L_2(\Omega)$.

Lemma 4.13. *Let u be the variational solution to (4.17) with a right-hand side $f \in L_2(\Omega)$. Then, Assumption 4.1 (ii) is satisfied. In particular, it holds $D^\alpha u_S(x, y) = \mathcal{O}(r(x, y)^{1+0.54-j})$ and $D^\alpha u_R(x, y) = \mathcal{O}(r(x, y)^{2-j})$, $|\alpha| = j$, $j = 0, 1, 2$, $r \rightarrow 0$.*

By (4.18), the statement for u_S is obvious. The proof of the result for the regular part u_R works in a completely analogous way to the proof of Lemma 4.9 and can therefore be omitted.

Finally, an application of Theorem 4.5 yields the following final result.

Corollary 4.14. *Let u be the variational solution to (4.17) with a right-hand side $f \in L_2(\Omega)$. Then, the sequence of frame coefficients $(2^{2|\lambda|} \langle u, \sigma_i \psi_{i,\lambda} \rangle)_{\lambda \in \mathcal{I}^\square, i=1,2}$ belongs to the space $\ell_{\tau_0}(\mathcal{I})$, where $\frac{1}{\tau_0} = \frac{s'-2}{2} + \frac{1}{2}$, for all $2 < s' < 2.64$.*

Proof. In order to be able to apply Theorem 4.5, one has to establish Besov regularity in the scale $\frac{1}{\tau} = \frac{s-(2+\delta)}{2} + \frac{1}{2}$ for a $\delta > 0$ and an $s > 2 + \delta$. To this end, note first that following the lines of [15], it can be shown that the variational solution u to problem (4.17) satisfies

$$u \in B_{\tau_1}^\alpha(L_{\tau_1}(\Omega)), \quad 0 < \alpha < 4, \quad \frac{1}{\tau_1} = \frac{\alpha}{2} + \frac{1}{2}. \quad (4.19)$$

[29, Theorem 1.2.18] and Lemma 4.13 imply $u \in H^{2+0.54}(\Omega)$. Now, using again interpolation between $H^{2.54}(\Omega)$ and $B_{\tau_1}^\alpha(L_{\tau_1}(\Omega))$, $0 < \alpha < 4$, $\frac{1}{\tau_1} = \frac{\alpha}{2} + \frac{1}{2}$, it is immediate to verify that, for any $\delta \in (0, 0.54)$, $u \in B_\tau^s(L_\tau(\Omega))$, where $\frac{1}{\tau} = \frac{s-(2+\delta)}{2} + \frac{1}{2}$, for all $s \in (2 + \delta, 2 + \delta + \frac{4(0.54-\delta)}{2.54})$. $g(\delta) := 2 + \delta + \frac{4(0.54-\delta)}{2.54}$ is a linear and decreasing function which on \mathbb{R}_+ attains its maximum $2 + \frac{4 \cdot 0.54}{2.54} > 2.85$ for $\delta = 0$. That means that the regularity index s in Theorem 4.5 can be chosen equal to 2.85, if δ is chosen sufficiently small.

Furthermore, it is important to note that the parameter η in Theorem 4.5 is given by Proposition 4.2, i.e., by $u_i \in H^{2+\eta}(\Omega)$, $i = 1, 2$, for some sufficiently small $\eta > 0$. In particular, reconsidering the proof of Proposition 4.2 for the present special case, we learn that, for $|\alpha| = 2$, $(\phi \circ \theta) D^\alpha u \in H^{\tilde{\nu}}(\Omega)$ for all $\tilde{\nu} < 0.54$. Moreover, (4.12) reads as $p < \frac{2}{1.46} < 2$, and hence the rightmost sum in (4.11) is contained in $H^{1-2(\frac{1}{p}-\frac{1}{2})}(\Omega)$ for all $p < \frac{2}{1.46}$. Thus, $u_i \in H^{2+\tilde{\nu}}(\Omega)$ for all $\tilde{\nu} < 0.54$, $i = 1, 2$. Finally, an application of Theorem 4.5 with $t = 2$, $s = 2.85$, and $\eta \in (0, 0.54)$ completes the proof. \square

5 New Boundary Adapted Wavelets on the Interval

The results of the previous section are essential for a classification of an adaptive scheme in terms of the error of approximation in relation to the number of unknowns. But in a practical implementation also the quantitative performance is very important. It depends on the constants involved in the error estimates used in the convergence analysis. The most important quantity in this context is the spectral condition of the stiffness matrix \mathbf{G} , see [19, 38]. Its value depends on the properties of the underlying aggregated frame, and therefore, it can be influenced by an appropriate choice of the reference systems $\Psi^{(i)}$. The latter bases are usually obtained by tensor products of wavelet bases on the interval.

Therefore, in this section, we present a new construction for biorthogonal wavelet bases on the interval that has recently been developed in [34]. It has been shown there that these bases exhibit good Riesz constants and give rise to well conditioned stiffness matrices stemming from 1D Poisson problems. Thus, one can expect that using the new bases as basic building block for the construction of wavelet frames on domains, should lead to well conditioned stiffness matrices arising in wavelet frame discretizations of operator equations.

The construction is based on biorthogonal MRAs using the Cohen-Daubechies-Feauveau scaling functions on \mathbb{R} (cp. [11]) as point of departure. The primal multiresolution will consist of spline spaces of order d , whereas the the dual multiresolution will have order \tilde{d} of polynomial exactness. One important feature of the construction is that the primal multiresolution consists of the well known Schoenberg-spline spaces of order d corresponding to equidistant knots on $[0, 1]$, where the boundary knots have multiplicity d . Therefore, no boundary adaption has to be done for the primal scaling functions. Furthermore, the dual scaling functions are constructed in a way that they will have staggered supports. For the derivation of the associated wavelet bases on the interval, we use the method of stable completion. Combined with our approach for the MRAs, this leads to a very low number of boundary wavelets.

Throughout this section, we focus on the special case $d = 3$, $\tilde{d} \geq 3$, \tilde{d} odd. Moreover, in view of the applications we have in mind, we only consider the case where the primal bases satisfy homogeneous boundary conditions, and no boundary conditions are imposed on the dual side. A more general construction is presented in [34].

5.1 Biorthogonal Scaling Functions on \mathbb{R}

We recapitulate the fundamental properties of the well known CDF-scaling functions for the case $d = 3$ and arbitrary odd $\tilde{d} \geq 3$. Let ϕ be the cardinal quadratic B-spline and $\tilde{\phi}$ as defined in [11]. Then the following properties hold:

1. **Compact support:** $\text{supp } \phi = [-1, 2]$, $\text{supp } \tilde{\phi} = [-\tilde{d}, \tilde{d} + 1]$.
2. **Normalization:** $\int_{\mathbb{R}} \phi(x) dx = \int_{\mathbb{R}} \tilde{\phi}(x) dx = 1$.
3. **Symmetry:** All scaling functions are symmetric around a half.
4. **Duality:** $\langle \phi, \tilde{\phi}(\cdot - m) \rangle_{L_2(\mathbb{R})} \delta_{0,m}$, where $\langle \cdot, \cdot \rangle_{L_2(\mathbb{R})}$ denotes the $L_2(\mathbb{R})$ scalar product.

5. **Polynomial exactness:** The function ϕ is exact of order 3, i.e. there exist for $r = 0, 1, 2$, $m \in \mathbb{Z}$ coefficients $\tilde{\alpha}_{m,r}$, such that

$$x^r = \sum_{m \in \mathbb{Z}} \tilde{\alpha}_{m,r} \phi(x - m) \text{ for all } x \in \mathbb{R}.$$

The functions $\tilde{\phi}$ are exact of order \tilde{d} , i.e. there exist for $r = 0, \dots, \tilde{d} - 1$, $m \in \mathbb{Z}$, coefficients $\alpha_{m,r}$, such that

$$x^r = \sum_{m \in \mathbb{Z}} \alpha_{m,r} \tilde{\phi}(x - m) \text{ for all } x \in \mathbb{R}.$$

Example 5.1. For the case $\tilde{d} = 5$ the scaling functions have the following shape:

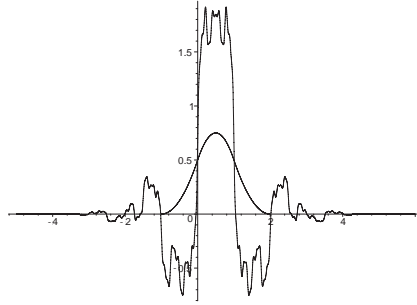


Figure 4: Primal and dual scaling function for $\tilde{d} = 5$

5.2 The Primal MRA on the Interval

In this section we present the primal quadratic spline MRA on the interval $[0, 1]$ with homogeneous boundary conditions of order one. It is associated with the the primal MRA on \mathbb{R} in Section 5.1.

For $j \in \mathbb{N}_{\geq 2}$ set $T^j := \{t_k^j\}_{k=-1}^{2^j+1}$ with

$$\begin{aligned} t_{-2+k}^j &= 0, & k &= 1, \dots, 2 \\ t_k^j &= 2^{-j}k, & k &= 1, \dots, 2^j - 1 \\ t_{2^j+k}^j &= 1, & k &= 1, \dots, 2 \end{aligned}$$

The B-splines

$$B_k^j(x) := (t_{k+3}^j - t_k^j)[t_k^j, \dots, t_{k+3}^j; (t-x)_+^2]_t, \quad k = -1, \dots, 2^j - 2 \quad (5.1)$$

with $(t-x)_+ := \max\{t-x, 0\}$ form a basis of the spline space

$$S^{(1)}(3, T^j) := \{f \in C^1([0, 1]) \mid f|_{[t_k^j, t_{k+1}^j]} \in P_3([t_k^j, t_{k+1}^j]), f(0) = f(1) = 0\}$$

with boundary conditions of order one. Here $P_m([a, b])$ denotes the space of all polynomials up to degree $m - 1$ on the interval $[a, b]$.

Let us summarize some familiar properties of the B_k^j , $k = -1, \dots, 2^j - 2$, cf. [37]:

1. (Compact support) $\text{supp } B_k^j = [t_k^j, t_{k+1}^j]$
2. (Symmetry) $B_k^j = B_{2^j-3-k}^j(1 - \cdot)$ for all $k = -1, \dots, 2^j - 2$
3. For the quadratic cardinal B-spline ϕ we get for $j \geq 2$, $k = 1, \dots, 2^j - 2$

$$\phi_{j,k} = 2^{\frac{j}{2}} \phi(2^j \cdot -k) = 2^{\frac{j}{2}} B_{k-1}^j. \quad (5.2)$$

4. $B_{-1}^{j+1} = B_{-1}^j(2 \cdot)$

As basis for the primal MRA we now choose the set

$$\Phi_j := \{2^{\frac{j}{2}} B_k^j : k = -1, \dots, 2^j - 2\}$$

and define the space

$$V_j := S^{(1)}(3, T^j) = \text{span } \Phi_j. \quad (5.3)$$

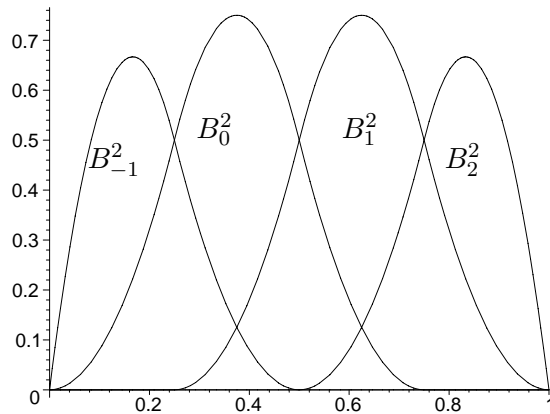


Figure 5: The B-Splines B_k^2 for $k = -1, \dots, 2$

Remark 5.2. It is well known (see e.g. [8, 34, 42]), that the sequence $\{V_j\}_{j \geq 2}$ is a *Multiresolution Analysis* (MRA) for the space $L_2([0, 1])$. In particular, there exist matrices $\mathbf{M}_{j,0} \in \mathbb{R}^{2^{j+1} \times 2^j}$, such that

$$\Phi_j^T = \Phi_{j+1}^T \mathbf{M}_{j,0}.$$

ii) $\langle \phi(\cdot - k), \tilde{\phi}_{\tilde{d}-1-n} \rangle_{\mathbb{R}_0^+} = 0$ for $k \geq \tilde{d}$. (Orthogonality)

iii) There exist two-scale-coefficients $\tilde{m}_{n,k}^L$ such that

$$\tilde{\phi}_k^L = \sum_{n=0}^{\tilde{d}-1} \tilde{m}_{n,k}^L \tilde{\phi}_n^L(2\cdot) + \sum_{n=\tilde{d}}^{3\tilde{d}-2k-1} \tilde{m}_{n,k}^L \tilde{\phi}(2\cdot - n). \quad (\text{Refinement Relation})$$

Proof: Statement i) directly follows from $\text{supp } \tilde{\phi} = [-\tilde{d}, \tilde{d} + 1]$ and (5.5).

For ii) we get

$$\begin{aligned} \langle \phi(\cdot - k), \tilde{\phi}_{\tilde{d}-1-n}^L \rangle_{\mathbb{R}_0^+} &= \sum_{m=n}^{2\tilde{d}-1} \binom{m}{n} \langle \phi(\cdot - k), \tilde{\phi}(\cdot + m - \tilde{d} + 1) \rangle_{\mathbb{R}_0^+} \\ &= \sum_{m=n}^{2\tilde{d}-1} \binom{m}{n} \langle \phi(\cdot - k), \tilde{\phi}(\cdot + m - \tilde{d} + 1) \rangle_{\mathbb{R}} \\ &= \sum_{m=n}^{2\tilde{d}-1} \binom{m}{n} \delta_{m-\tilde{d}+1,k} = 0, \end{aligned}$$

since $-k \leq -\tilde{d} < -\tilde{d} + 1 \leq m - \tilde{d} + 1$ for all $m = n, \dots, 2\tilde{d} - 1$.

We abandon the proof of statement iii) and refer to [12, 34]. For two-scale-coefficients we use in our application will be presented below. □

We return to the situation on the interval and set for $j \geq j_0$ at the left boundary

$$\tilde{\Phi}_j^L := \{\tilde{\phi}_{j,k}^L : k = 0, \dots, \tilde{d} - 1\} \quad \text{with} \quad \tilde{\phi}_{j,k}^L := 2^{\frac{j}{2}} \tilde{\phi}_k^L(2^j \cdot)$$

and symmetrically at the right boundary

$$\tilde{\Phi}_j^R := \{\tilde{\phi}_{j,k}^R : k = 0, \dots, \tilde{d} - 1\} \quad \text{with} \quad \tilde{\phi}_{j,k}^R := \tilde{\phi}_{j,k}^L(1 - \cdot).$$

Further, we define

$$\tilde{\Phi}_j := \tilde{\Phi}_j^L \cup \tilde{\Phi}_j^I \cup \tilde{\Phi}_j^R. \quad (5.6)$$

On the primal side we subdivide the set Φ_j analogously into

$$\Phi_j = \Phi_j^L \cup \Phi_j^I \cup \Phi_j^R,$$

where

$$\Phi_j^L := \{2^{\frac{j}{2}} B_k^j : k = -1, \dots, \tilde{d} - 2\}, \quad \Phi_j^R := \{2^{\frac{j}{2}} B_k^j : k = 2^j - \tilde{d} - 1, \dots, 2^j - 2\}$$

and

$$\Phi_j^I := \{2^{\frac{j}{2}} B_k^j : \tilde{d} - 1, \dots, 2^j - \tilde{d} - 2\} = \{\phi_{j,k} : k = \tilde{d}, \dots, 2^j - \tilde{d} - 1\}.$$

Note, that in Φ_j^L only the function $2^{\frac{j}{2}} B_{-1}^j$ is a real boundary function, the others actually coincide with the inner functions $\phi_{j,k}$, $k = 1, \dots, \tilde{d} - 1$ (cp. (5.2)).

Lemma 5.4. *Let $\Phi_j, \tilde{\Phi}_j$ be defined as above. Then for $j \geq j_0$ the following properties hold.*

- i) $\langle \Phi_j^L, \tilde{\Phi}_j^I \rangle_{[0,1]} = \langle \Phi_j^R, \tilde{\Phi}_j^I \rangle_{[0,1]} = \langle \Phi_j^I, \tilde{\Phi}_j^L \rangle_{[0,1]}^T = \langle \Phi_j^I, \tilde{\Phi}_j^R \rangle_{[0,1]}^T = \mathbf{0}$,
- ii) $\langle \Phi_j^L, \tilde{\Phi}_j^R \rangle_{[0,1]} = \langle \Phi_j^R, \tilde{\Phi}_j^L \rangle_{[0,1]} = \mathbf{0}$,
- iii) $\langle \Phi_j^I, \tilde{\Phi}_j^I \rangle_{[0,1]} = \mathbf{I}_{2^j - 2\tilde{d}}$.

Proof: It can be shown, that the primal boundary functions are linear combinations of functions $\phi_{j,k}$ restricted to the interval, where the functions from Φ_j^I are not used. The same is valid for the dual boundary functions. Thus, the biorthogonality of the functions $\phi_{j,k}, \tilde{\phi}_{j,k}$ proves the assertions i) - iii). \square

5.3.2 Biorthogonalization

Up to now we have not considered the biorthogonality of the bases $\Phi_j, \tilde{\Phi}_j$. While we have the identities i) from Lemma 5.4, the boundary functions $\Phi_j^L, \tilde{\Phi}_j^L$ are not biorthogonal. The same is valid for the boundary functions on the right hand side. We consider the left side case and set

$$\Gamma^L := \langle \Phi_j^L, \tilde{\Phi}_j^L \rangle_{[0,1]}.$$

The matrix Γ^L can be determined with the methods presented in [12, 33, 34]. Note, that Γ^L is independent of j . We get the matrix $\Gamma^R := \langle \Phi_j^R, \tilde{\Phi}_j^R \rangle_{[0,1]}$ by inverting the order of the rows and columns of Γ^L . The main challenge is now to show, that Γ^L is in fact invertible, so that a biorthogonalization is possible and that it does not destroy the staggeredness of the supports of the dual boundary functions. In [34] it is shown, that the matrix Γ^L is for all appropriate \tilde{d} a regular upper triangular matrix with determinant $\frac{2}{\tilde{d}+2}$.

Example 5.5. For $\tilde{d} = 3, 5$ we find

$$\Gamma_3^L = \begin{bmatrix} \frac{2}{5} & \frac{7}{6} & \frac{2}{3} \\ 0 & 1 & 1 \\ 0 & 0 & 1 \end{bmatrix}, \quad \Gamma_5^L = \begin{bmatrix} \frac{2}{7} & \frac{19}{10} & \frac{17}{5} & \frac{5}{2} & \frac{2}{3} \\ 0 & 1 & 3 & 3 & 1 \\ 0 & 0 & 1 & 2 & 1 \\ 0 & 0 & 0 & 1 & 1 \\ 0 & 0 & 0 & 0 & 1 \end{bmatrix}.$$

We now set

$$(\tilde{\Phi}_j^L)^{new} := (\Gamma^L)^{-T} \Phi_j^L,$$

such that

$$\langle \Phi_j^L, (\tilde{\Phi}_j^L)^{new} \rangle_{[0,1]} = \Phi_j^L ((\tilde{\Phi}_j^L)^{new})^T = \left[\Phi_j^L (\tilde{\Phi}_j^L)^T \right] (\Gamma^L)^{-1} = \Gamma^L (\Gamma^L)^{-1} = \mathbf{I}_{\tilde{d}}.$$

On the right hand side we set analogously $(\tilde{\Phi}_j^R)^{new} := (\Gamma^R)^{-T} \Phi_j^R$.

Using this transform, the primal basis remains unchanged while at the dual side the former boundary functions are recombined to new boundary functions, which are biorthogonal to the primal side. Note, that due to the structure of Γ^L, Γ^R the supports of the new dual boundary functions are still staggered after biorthogonalization.

Remark 5.6. In contrast to (5.6) we now redefine

$$\tilde{\Phi}_j := (\tilde{\Phi}_j^L)^{new} \cup \tilde{\Phi}^I \cup (\tilde{\Phi}_j^R)^{new}$$

as the set of biorthogonalized dual scaling functions. From now on we only use the biorthogonalized version and set in analogy to (5.3)

$$\tilde{V}_j := \text{span } \tilde{\Phi}_j.$$

It can be shown that for the spaces \tilde{V}_j appropriate two-scale relations hold. In particular, cf. [23, 34], there exist matrices $\tilde{\mathbf{M}}_{j,0} \in \mathbb{R}^{2^{j+1} \times 2^j}$, such that

$$\tilde{\Phi}_j^T = \tilde{\Phi}_{j+1}^T \tilde{\mathbf{M}}_{j,0}.$$

For the cases $\tilde{d} = 3, 5$, the matrices $\tilde{\mathbf{M}}_{j,0}$ are given below.

Example 5.7. After biorthogonalization, for the case $\tilde{d} = 3$ and $j = 3$ we get the two-scale-matrix

$$\tilde{M}_{3,0} = \frac{1}{\sqrt{2}} \begin{bmatrix} \frac{29}{16} & -\frac{67}{96} & \frac{5}{32} & 0 & 0 & 0 & 0 & 0 & 0 \\ \frac{45}{32} & \frac{7}{64} & -\frac{3}{64} & 0 & 0 & 0 & 0 & 0 & 0 \\ \frac{5}{32} & \frac{205}{192} & -\frac{11}{64} & 0 & 0 & 0 & 0 & 0 & 0 \\ -\frac{45}{64} & \frac{213}{128} & -\frac{37}{128} & \frac{3}{32} & 0 & 0 & 0 & 0 & 0 \\ \frac{15}{64} & -\frac{39}{128} & \frac{183}{128} & -\frac{9}{32} & 0 & 0 & 0 & 0 & 0 \\ 0 & -\frac{9}{32} & \frac{45}{32} & -\frac{7}{32} & \frac{3}{32} & 0 & 0 & 0 & 0 \\ 0 & \frac{3}{32} & -\frac{7}{32} & \frac{45}{32} & -\frac{9}{32} & 0 & 0 & 0 & 0 \\ 0 & 0 & -\frac{9}{32} & \frac{45}{32} & -\frac{7}{32} & \frac{3}{32} & 0 & 0 & 0 \\ 0 & 0 & \frac{3}{32} & -\frac{7}{32} & \frac{45}{32} & -\frac{9}{32} & 0 & 0 & 0 \\ 0 & 0 & 0 & -\frac{9}{32} & \frac{45}{32} & -\frac{7}{32} & \frac{3}{32} & 0 & 0 \\ 0 & 0 & 0 & \frac{3}{32} & -\frac{7}{32} & \frac{45}{32} & -\frac{9}{32} & 0 & 0 \\ 0 & 0 & 0 & 0 & -\frac{9}{32} & \frac{183}{128} & -\frac{39}{128} & \frac{15}{64} & 0 \\ 0 & 0 & 0 & 0 & \frac{3}{32} & -\frac{37}{128} & \frac{213}{128} & -\frac{45}{64} & 0 \\ 0 & 0 & 0 & 0 & 0 & -\frac{11}{64} & \frac{205}{192} & \frac{5}{32} & 0 \\ 0 & 0 & 0 & 0 & 0 & -\frac{3}{64} & \frac{7}{64} & \frac{45}{32} & 0 \\ 0 & 0 & 0 & 0 & 0 & \frac{5}{32} & -\frac{67}{96} & \frac{29}{16} & 0 \end{bmatrix}$$

For the case $\tilde{d} = 5$ the left edge boundary block of $\tilde{M}_{4,0}$ has the entries

$$\left((\tilde{M}_{4,0})_{n,m} \right)_{n,m=1}^{15,5} = \frac{1}{\sqrt{2}} \begin{bmatrix} \frac{281}{128} & -\frac{1731}{1280} & \frac{1047}{1280} & -\frac{203}{640} & \frac{7}{128} \\ \frac{315}{256} & \frac{211}{512} & -\frac{183}{512} & \frac{39}{256} & -\frac{7}{256} \\ -\frac{21}{256} & \frac{3759}{2560} & -\frac{1443}{2560} & \frac{227}{1280} & -\frac{7}{256} \\ -\frac{77}{256} & \frac{2583}{2560} & \frac{789}{2560} & -\frac{181}{1280} & \frac{19}{768} \\ -\frac{21}{256} & \frac{399}{2560} & \frac{2877}{2560} & -\frac{333}{1280} & \frac{9}{256} \\ \frac{105}{512} & -\frac{547}{1024} & \frac{1523}{1024} & -\frac{79}{512} & \frac{43}{512} \\ -\frac{35}{512} & \frac{129}{1024} & -\frac{145}{1024} & \frac{709}{512} & -\frac{587}{1536} \\ 0 & \frac{15}{256} & -\frac{97}{256} & \frac{175}{128} & -\frac{13}{128} \\ 0 & -\frac{5}{256} & \frac{19}{256} & -\frac{13}{128} & \frac{175}{128} \\ 0 & 0 & \frac{15}{256} & -\frac{97}{256} & \frac{175}{128} \\ 0 & 0 & -\frac{5}{256} & \frac{19}{256} & -\frac{13}{128} \\ 0 & 0 & 0 & \frac{15}{256} & -\frac{97}{256} \\ 0 & 0 & 0 & -\frac{5}{256} & \frac{19}{256} \\ 0 & 0 & 0 & 0 & \frac{15}{256} \\ 0 & 0 & 0 & 0 & -\frac{5}{256} \end{bmatrix}$$

The biorthogonalized boundary functions for $\tilde{d} = 5$, $j = 0$ are shown in Figure 3.

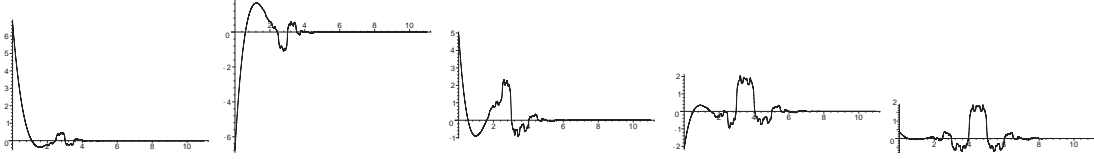


Figure 6: The left edge boundary functions after biorthogonalization for $\tilde{d} = 5$, $j = 0$.

5.3.3 Polynomial Exactness and Regularity

In the following Lemma we point out some important properties of the bases $\{\Phi_j\}_{j \geq j_0}$, $\{\tilde{\Phi}_j\}_{j \geq j_0}$.

Lemma 5.8. *Let $\Phi_j, \tilde{\Phi}_j$, $j \geq j_0$ be the biorthogonal bases, defined as below. Then the following properties hold.*

- i) *The sets Φ_j are locally exact of order d , i.e. all polynomials up to degree $d - 1$ can be reproduced on the interval $[2^{-j}, 1 - 2^{-j}]$. The sets $\tilde{\Phi}_j$ are exact of order \tilde{d} , i.e. $P_{\tilde{d}}([0, 1]) \subset \tilde{V}_j$.*
- ii) *We have $\Phi_j \subset H^s([0, 1]) \cap H_0^1([0, 1])$ for all $s < \frac{5}{2}$, i.e. $\|\varphi_j\|_{H^s([0, 1])} \lesssim 2^{sj}$ for all $\varphi \in \Phi_j$. For all \tilde{d} we find a $\tilde{\gamma} > 0$ such that $\tilde{\Phi}_j \subset H^{\tilde{s}}([0, 1])$ for all $\tilde{s} < \tilde{\gamma}$, i.e. $\|\tilde{\varphi}_j\|_{H^{\tilde{s}}([0, 1])} \lesssim 2^{\tilde{s}j}$ for all $\tilde{\varphi}_j \in \tilde{\Phi}_j$.*

Proof: To i): The local exactness of Φ_j is a well known result from spline theory and we refer to [37]. The proof of the polynomial exactness of $\tilde{\Phi}_j$ (cg. [34]) is analogous to the considerations in [12, 23].

To *ii*): The Sobolev regularity of the functions $\phi, \tilde{\phi}$ is well known. Since the boundary functions are linear combinations of these functions restricted to the interval the assertion *ii*) can be proved with the methods from [21, 22]. \square

Remark 5.9. From Lemma 5.8 one can infer that the sequences $(V_j)_{j \geq j_0}$ and $(\tilde{V}_j)_{j \geq j_0}$ both form an MRA for $L_2([0, 1])$, cf. [23, 34].

Remark 5.10. A numerical determination of $\tilde{\gamma}$ yields $\tilde{\gamma} \approx 0.175$ for $\tilde{d} = 3$, $\tilde{\gamma} \approx 0.793$ for $\tilde{d} = 5$ and $\tilde{\gamma} \approx 1.344$ for $\tilde{d} = 7$ (cg. [11, 31]).

5.4 Construction of the Wavelets

5.4.1 The Method of Stable Completion

The derivation of the wavelets is accomplished with the method of stable completion. We do not explain this method here in detail, but refer to [6, 23, 34]. The method in [34], which is also used here, is slightly modified in order to increase the number of inner wavelets. The main idea of the stable completion is to find matrices $\mathbf{M}_{j,1}, \tilde{\mathbf{M}}_{j,1}$, such that for $j \geq j_0$ the sets

$$\Psi_j^T := \Phi_{j+1}^T \mathbf{M}_{j,1}, \quad \tilde{\Psi}_j^T := \tilde{\Phi}_{j+1}^T \tilde{\mathbf{M}}_{j,1}$$

form a biorthogonal system with

$$\langle \Psi_j, \tilde{\Psi}_j \rangle = \mathbf{I}, \langle \Psi_j, \tilde{\Phi}_j \rangle = \langle \Phi_j, \tilde{\Psi}_j \rangle = \mathbf{0}.$$

Note, that the method of stable completion as presented in [6, 23, 34] automatically provides the wavelets from [11] as inner wavelets added by a certain number of boundary wavelets. A proof for this assertion is given in [34].

Example 5.11. For the case $\tilde{d} = 3$ the method of stable completion produces for $j = 3$ the matrices

$$M_{3,1} := \frac{1}{\sqrt{2}} \begin{bmatrix} -\frac{315}{256} & -\frac{15}{32} & 0 & 0 & 0 & 0 & 0 & 0 & 0 \\ \frac{1365}{1024} & -\frac{15}{128} & -\frac{3}{32} & 0 & 0 & 0 & 0 & 0 & 0 \\ -\frac{81}{1024} & \frac{195}{128} & -\frac{9}{32} & 0 & 0 & 0 & 0 & 0 & 0 \\ -\frac{279}{512} & -\frac{75}{64} & \frac{7}{32} & -\frac{3}{32} & 0 & 0 & 0 & 0 & 0 \\ -\frac{33}{512} & -\frac{13}{64} & \frac{45}{32} & -\frac{9}{32} & 0 & 0 & 0 & 0 & 0 \\ \frac{135}{1024} & \frac{27}{128} & -\frac{45}{32} & \frac{7}{32} & \frac{3}{32} & 0 & 0 & 0 & 0 \\ \frac{45}{1024} & \frac{9}{128} & -\frac{7}{32} & \frac{45}{32} & \frac{9}{32} & 0 & 0 & 0 & 0 \\ 0 & 0 & \frac{9}{32} & -\frac{45}{32} & -\frac{7}{32} & \frac{3}{32} & 0 & 0 & 0 \\ 0 & 0 & \frac{3}{32} & -\frac{7}{32} & -\frac{45}{32} & \frac{9}{32} & 0 & 0 & 0 \\ 0 & 0 & 0 & \frac{9}{32} & \frac{45}{32} & -\frac{7}{32} & \frac{9}{128} & \frac{45}{1024} & 0 \\ 0 & 0 & 0 & \frac{3}{32} & \frac{7}{32} & -\frac{45}{32} & \frac{27}{128} & \frac{135}{1024} & 0 \\ 0 & 0 & 0 & 0 & -\frac{9}{32} & \frac{45}{32} & -\frac{13}{64} & -\frac{33}{512} & 0 \\ 0 & 0 & 0 & 0 & -\frac{3}{32} & \frac{7}{32} & -\frac{75}{64} & -\frac{279}{512} & 0 \\ 0 & 0 & 0 & 0 & 0 & -\frac{9}{32} & \frac{195}{128} & -\frac{81}{1024} & 0 \\ 0 & 0 & 0 & 0 & 0 & -\frac{3}{32} & -\frac{15}{128} & \frac{1365}{1024} & 0 \\ 0 & 0 & 0 & 0 & 0 & 0 & -\frac{15}{32} & -\frac{315}{256} & 0 \end{bmatrix}$$

and

$$\tilde{M}_{3,1} := \frac{1}{\sqrt{2}} \begin{bmatrix} -\frac{8}{9} & 0 & 0 & 0 & 0 & 0 & 0 & 0 \\ \frac{2}{3} & -\frac{1}{4} & 0 & 0 & 0 & 0 & 0 & 0 \\ -\frac{2}{9} & \frac{3}{4} & 0 & 0 & 0 & 0 & 0 & 0 \\ 0 & -\frac{3}{4} & -\frac{1}{4} & 0 & 0 & 0 & 0 & 0 \\ 0 & \frac{1}{4} & \frac{3}{4} & 0 & 0 & 0 & 0 & 0 \\ 0 & 0 & -\frac{3}{4} & -\frac{1}{4} & 0 & 0 & 0 & 0 \\ 0 & 0 & \frac{1}{4} & \frac{3}{4} & 0 & 0 & 0 & 0 \\ 0 & 0 & 0 & -\frac{3}{4} & \frac{1}{4} & 0 & 0 & 0 \\ 0 & 0 & 0 & \frac{1}{4} & -\frac{3}{4} & 0 & 0 & 0 \\ 0 & 0 & 0 & 0 & \frac{3}{4} & \frac{1}{4} & 0 & 0 \\ 0 & 0 & 0 & 0 & -\frac{1}{4} & -\frac{3}{4} & 0 & 0 \\ 0 & 0 & 0 & 0 & 0 & \frac{3}{4} & \frac{1}{4} & 0 \\ 0 & 0 & 0 & 0 & 0 & -\frac{1}{4} & -\frac{3}{4} & 0 \\ 0 & 0 & 0 & 0 & 0 & 0 & \frac{3}{4} & -\frac{2}{9} \\ 0 & 0 & 0 & 0 & 0 & 0 & -\frac{1}{4} & \frac{2}{3} \\ 0 & 0 & 0 & 0 & 0 & 0 & 0 & -\frac{8}{9} \end{bmatrix},$$

so that we have three boundary wavelets at the primal side and two boundary wavelets at the dual side. For $\tilde{d} = 5$ we find for $j \geq 4$

$$\left((M_{j,1})_{n,m} \right)_{n,m=1}^{11,3} := \frac{1}{\sqrt{2}} \begin{bmatrix} -\frac{2079}{2048} & -\frac{63}{256} & \frac{35}{256} \\ \frac{60291}{40960} & \frac{147}{5120} & \frac{21}{1024} \\ -\frac{21447}{40960} & \frac{5481}{5120} & -\frac{497}{1024} \\ -\frac{18657}{20480} & -\frac{3969}{2560} & -\frac{7}{512} \\ \frac{1269}{4096} & \frac{85}{512} & \frac{735}{512} \\ -\frac{4923}{8192} & \frac{699}{1024} & -\frac{1295}{1024} \\ -\frac{1539}{40960} & -\frac{3}{5120} & -\frac{117}{1024} \\ -\frac{2583}{10240} & -\frac{311}{1280} & \frac{253}{768} \\ -\frac{441}{10240} & -\frac{57}{1280} & \frac{17}{256} \\ \frac{189}{4096} & \frac{21}{512} & -\frac{25}{512} \\ \frac{63}{4096} & \frac{7}{512} & -\frac{25}{1536} \end{bmatrix}$$

and

$$\left((\tilde{M}_{j,1})_{n,m} \right)_{n,m=1}^{11,3} := \frac{1}{\sqrt{2}} \begin{bmatrix} -\frac{8}{9} & 0 & 0 \\ \frac{2}{3} & -\frac{1}{4} & 0 \\ -\frac{2}{9} & \frac{3}{4} & 0 \\ 0 & -\frac{3}{4} & -\frac{1}{4} \\ 0 & \frac{1}{4} & \frac{3}{4} \\ 0 & 0 & -\frac{3}{4} \\ 0 & 0 & \frac{1}{4} \\ 0 & 0 & 0 \\ 0 & 0 & 0 \\ 0 & 0 & 0 \\ 0 & 0 & 0 \end{bmatrix},$$

where we have three boundary wavelets at each boundary at the primal and the dual side.

Remark 5.12. The original wavelets $\psi, \tilde{\psi}$ from [11] have support width $\tilde{d} + 2$. Since the number of possible inner wavelets is thus $2^j - \tilde{d} - 1$, the minimal number of wavelets, that have to be added per boundary is $\frac{\tilde{d}+1}{2}$. So we see, that for $\tilde{d} = 3$ the number of added boundary wavelets is almost minimal and for $\tilde{d} = 5$ minimal. As a comparison, the construction in [23] yields for example in the case $\tilde{d} = 5$ the number of 6 additional wavelets on the primal side and 4 additional wavelets at the dual side. Due to low condition numbers and good stability, the number of wavelets, that do not coincide with inner wavelets should be as small as possible. In this point of view our construction is nearly optimal.

5.4.2 Stability

We finally set $\Psi_{j_0-1} := \Phi_{j_0}$, $\tilde{\Psi}_{j_0-1} := \tilde{\Phi}_{j_0}$ and

$$\Psi := \bigcup_{j=j_0-1}^{\infty} \Psi_j, \quad \tilde{\Psi} := \bigcup_{j=j_0-1}^{\infty} \tilde{\Psi}_j.$$

Now, the most important question is, whether the sets $\Psi, \tilde{\Psi}$ are really biorthogonal Riesz bases, i.e.

$$\|\Psi^T c\|_{L_2([0,1])} \sim \|\tilde{\Psi}^T c\|_{L_2([0,1])} \sim \|c\|_2$$

for all sequences $c \in l_2(\mathbb{Z})$. Using the methods from [21, 22, 24] in [34] it is shown, that the MRAs $\{\Phi_j\}_{j \geq j_0}$ and $\{\tilde{\Phi}_j\}_{j \geq j_0}$ fulfill the required Bernstein- and Jackson estimates, such that the method of stable completion in fact leads to stable bases $\Psi, \tilde{\Psi}$. In especially, we have

$$\|v\|_{H_0^s([0,1])}^2 \sim \sum_{j=j_0-1}^{\infty} 2^{2sj} \|\langle v, \tilde{\Psi}_j \rangle_{[0,1]} \Psi_j\|_{L_2([0,1])}^2, \quad s \in (-\min\{\tilde{d}, \tilde{\gamma}\}, \frac{5}{2}),$$

with $\tilde{\gamma}$ from Remark 5.10. Thus, we can actually characterize a certain scale of Sobolev spaces with the aid of $\Psi, \tilde{\Psi}$.

5.5 Boundary Conditions of Higher Order

Finally, we make some remarks on the use of the previous approach for the construction of bases with Dirichlet boundary conditions of higher order. The primal MRA as presented in Section 5.2 has boundary condition of order one. If we skip the two outermost splines $2^{\frac{j}{2}} B_{-1}^j, 2^{\frac{j}{2}} B_{2^j-2}^j$, the sets $\text{span}\{2^{\frac{j}{2}} B_k^j : k = 0, \dots, 2^j - 3\}$ build a MRA of $L_2([0, 1])$ with boundary conditions of order two, i.e. $(B_k^j)^{(s)}(0) = (B_k^j)^{(s)}(1) = 0$ for $s = 0, 1$. Two-scale relation, local polynomial exactness in $[2^{-j+1}, 1 - 2^{-j+1}]$ and regularity remain the same as for Φ_j . To be more precise, in this case we only use the inner functions $\phi_{j,k}$, $k = 1, \dots, 2^j - 2$. Now we have to adapt the construction of the dual side as well. Since the number of scaling functions on the primal side is now $2^j - 2$, we also have to neglect two functions at the dual side. Due to the fact, that we want to preserve polynomial exactness of order \tilde{d} , we cannot skip a boundary function, but can withdraw the outermost inner functions $\tilde{\phi}_{j,\tilde{d}}, \tilde{\phi}_{j,2^j-\tilde{d}-1}$ (cp. (5.4)). They then have to be included into the boundary functions. The approach

(5.5) simply changes into

$$\tilde{\phi}_{\tilde{d}-1-n}^L := \sum_{m=n}^{2\tilde{d}} \binom{m}{n} \tilde{\phi}(\cdot + m - \tilde{d})|_{\mathbb{R}_0^+}.$$

The rest of the construction is completely analogous.

5.6 Wavelet Bases On The Cube

After the construction of appropriate wavelet bases on the interval, it is a straightforward procedure to generate corresponding wavelet bases on the unit cube $\square := (0, 1)^n$ via tensor products. Here we will use the same notation as in [23, 24]. Introducing a third wavelet type parameter $e \in \{0, 1\}$ with

$$\psi_{j,e,k} := \begin{cases} \phi_{j,k}, & e = 0 \\ \psi_{j,k}, & e = 1 \end{cases}. \quad (5.7)$$

and the index sets

$$\mathcal{N}^\square := \left\{ (j, \mathbf{e}, \mathbf{k}) : \mathbf{e} \in \{0, 1\}^n, \mathbf{k} \in \bigotimes_{i=1}^n \nabla_{j,e_i} \right\}, \quad (5.8)$$

where $\nabla_{j,e}$ are the admissible translation parameters k on the level j for the wavelet type e

$$\nabla_{j,e} := \begin{cases} \{1, \dots, 2^j - 2\}, & e = 0 \\ \{0, \dots, 2^j - 1\}, & e = 1 \end{cases}, \quad (5.9)$$

the tensor product wavelets on the cube \square are simply given by

$$\psi_\lambda^\square(\mathbf{x}) := \prod_{i=1}^n \psi_{j,e_i,k_i}(x_i), \quad \mathbf{x} \in \square, \lambda = (j, \mathbf{e}, \mathbf{k}) \in \mathcal{N}^\square. \quad (5.10)$$

6 Adaptive Numerical Frame Schemes

The intention of this section is to compare the quantitative numerical performance of an adaptive numerical frame scheme for the solution of elliptic operator equations, when either the new wavelet bases from Section 5 or the bases constructed in [24] are employed as building block for the construction of an aggregated Gelfand frame. In this section, we consider elliptic operators $\mathcal{L} : H_0^1(\Omega) \rightarrow H^{-1}(\Omega)$ of order $2t = 2$, resulting from the variational formulation of Poisson problems on the interval $\Omega = (0, 1)$ or on a two-dimensional L-shaped domain $\Omega = (-1, 1)^2 \setminus [0, 1]^2$. For the discretization, we will use aggregated wavelet frames on suitable overlapping domain decompositions, as the union of wavelet bases Ψ^\square on $(0, 1)$ or $(0, 1)^2$ lifted to the subdomains. As such reference systems, tensor products of the biorthogonal spline wavelet bases of order $d = 3$ with complementary boundary conditions from Section 5 and [24] will be employed, such that the primal wavelets will have $\tilde{d} = 3$ vanishing moments.

In Section 4, we have analyzed the convergence order of a best N -term wavelet frame approximation of the solution of an elliptic operator equation like in (2.1). First of all, in the present section the construction of an adaptive numerical frame scheme for the solution of the linear system (2.20) from [19] will be briefly summarized, which realizes this *optimal* order of convergence in linear complexity $\mathcal{O}(N)$.

6.1 An Adaptive Steepest Descent Scheme

In [19, 38] it has been shown that, in principle, the infinite linear system (2.20) can be solved with well known iterative methods such as the *damped Richardson* or the *steepest descent* iteration. In this paper, we focus on the latter method, which, for a starting vector $\mathbf{w}^{(0)} \in \ell_2(\mathcal{I})$, reads as follows

```

for  $n = 0, \dots$ ,
   $\mathbf{r}^{(n)} := \mathbf{f} - \mathbf{G}\mathbf{w}^{(n)}$ ;
   $\mathbf{w}^{(n+1)} := \mathbf{w}^{(n)} + \frac{\langle \mathbf{r}^{(n)}, \mathbf{r}^{(n)} \rangle}{\langle \mathbf{G}\mathbf{r}^{(n)}, \mathbf{r}^{(n)} \rangle} \mathbf{r}^{(n)}$ ;
   $n = n + 1$ ;
endfor.

```

Due to the redundancy of a frame, although we assumed the operator \mathcal{L} to be boundedly invertible, the discrete operator \mathbf{G} generally has a nontrivial kernel, and thus the system (2.20) is underdetermined. But since, by Lemma 2.1, \mathbf{G} is boundedly invertible on its range, there exists a *unique* solution $\bar{\mathbf{u}} \in \text{ran}(\mathbf{G})$. Moreover, it is easy to prove that for $\mathbf{w}^{(0)} \in \text{ran}(\mathbf{G})$, the ideal iterates $\mathbf{w}^{(n)}$ indeed converge to $\bar{\mathbf{u}} \in \text{ran}(\mathbf{G})$.

Nevertheless, such a method cannot be implemented directly, since an infinite matrix and infinite sequences are involved. The conceptual outline to derive a practicable algorithm is to replace each application of the infinite stiffness matrix \mathbf{G} , as well as the infinite right-hand side \mathbf{f} by appropriate finite dimensional approximations. To this end, one typically uses a routine **APPLY** $[\mathbf{w}, \varepsilon] \rightarrow \mathbf{z}_\varepsilon$, which, for a finitely supported \mathbf{w} determines a finitely supported \mathbf{z}_ε with $\|\mathbf{G}\mathbf{w} - \mathbf{z}_\varepsilon\|_{\ell_2} \leq \varepsilon$. Basically, this is done by extracting significant columns of \mathbf{G} in the linear combination $\mathbf{G}\mathbf{w} = \sum_\lambda \mathbf{G}^{(\lambda)} \mathbf{w}_\lambda$, i.e., by extracting those columns $\mathbf{G}^{(\lambda)}$ that are multiplied with large coefficients (in modulus) \mathbf{w}_λ , and by computing finite approximations to each of the chosen columns within a tolerance depending on the size of the corresponding coefficient and the prescribed accuracy ε .

The right-hand side \mathbf{f} will be approximated by a routine **RHS** $[\varepsilon] \rightarrow \mathbf{f}_\varepsilon$. For $\varepsilon > 0$, this function has to compute a finitely supported \mathbf{f}_ε with $\|\mathbf{f} - \mathbf{f}_\varepsilon\|_{\ell_2} \leq \varepsilon$. Finally, in order to control the support lengths of the iterates, and thus also the computational cost, a third numerical routine **COARSE** $[\mathbf{w}, \varepsilon] \rightarrow \mathbf{w}_\varepsilon$ is used, which determines a finitely supported \mathbf{w}_ε , such that $\|\mathbf{w} - \mathbf{w}_\varepsilon\|_{\ell_2} \leq \varepsilon$, where again \mathbf{w} is assumed to be finitely supported. Essentially, this is realized by a thresholding step. For further details on the precise realization of the numerical routines, we refer to [2, 10, 38].

Using these functions, it has been demonstrated in [19] that, by replacing one ideal step of the above scheme with an approximation up to certain geometrically decreasing precisions ε_n , $n \rightarrow \infty$, an implementable adaptive algorithm **SOLVE** $[\omega, \varepsilon]$ can be derived. Here, the input parameter $\omega > 0$ configures the initial precision ε_0 . Since in such a scheme only perturbed steps of the former iteration are performed, the iterates may have nontrivial

components in the kernel of \mathbf{G} , which was not the case for the exact $\mathbf{w}^{(n)}$, provided that $\mathbf{w}^{(0)} \in \text{ran}(\mathbf{G})$. Such components, once occurred in an iterate and therefore in the residual, will never be reduced in subsequent steps. Nevertheless, the following result, stating convergence of the method, can be established.

Theorem 6.1 (see [19]). *Let \mathbf{Q} denote the ℓ_2 -orthogonal projection onto $\text{ran}(\mathbf{G})$. If $\omega \geq \|\bar{\mathbf{u}}\|_{\ell_2}$, then for any $\varepsilon > 0$, $\mathbf{SOLVE}[\omega, \varepsilon] =: \mathbf{w}_\varepsilon$ terminates with $\|\bar{\mathbf{u}} - \mathbf{Q}\mathbf{w}_\varepsilon\|_{\ell_2} \leq \varepsilon$.*

Observe that from $\|\bar{\mathbf{u}} - \mathbf{Q}\mathbf{w}_\varepsilon\|_{\ell_2} \leq \varepsilon$ it follows that also $\|u - F^*D^{-1}\mathbf{w}_\varepsilon\|_H \lesssim \varepsilon$, e.g., [18, 38]. Since furthermore $\ker(\mathbf{G}) = \ker(F^*D^{-1})$, the fact that $(\mathbf{I} - \mathbf{Q})\mathbf{w}_\varepsilon$ might be nontrivial does not spoil the convergence of the method.

However, the main result in [19] was to prove that \mathbf{SOLVE} converges with the best possible rate in linear complexity. In particular, assume that for some $s > 0$ there exists a solution \mathbf{u} to (2.1) satisfying

$$\sup_{N \in \mathbb{N}} N^s \sigma_N(\mathbf{u}) < \infty, \quad (6.1)$$

or equivalently $\mathbf{u} \in \ell_\tau^w(\mathcal{I})$, where $\tau = (s + \frac{1}{2})^{-1}$. Membership $\mathbf{u} \in \ell_\tau^w(\mathcal{I})$ implies that for any $\varepsilon > 0$ there exists a \mathbf{u}_ε such that

$$\#\text{supp } \mathbf{u}_\varepsilon \lesssim \varepsilon^{-1/s} |\mathbf{u}|_{\ell_\tau^w(\mathcal{I})}^{1/s}, \quad (6.2)$$

while $\|\mathbf{u} - \mathbf{u}_\varepsilon\|_{\ell_2(\mathcal{I})} \leq \varepsilon$. Additionally, suppose that for some s^* greater than any s for which $\mathbf{u} \in \ell_\tau^w(\mathcal{I})$ can be expected, the routine $\mathbf{APPLY}[\mathbf{w}, \varepsilon] \rightarrow \mathbf{z}_\varepsilon$ can be implemented in such a way that for any $\tilde{s} < s^*$, $\#\text{supp } \mathbf{z}_\varepsilon \lesssim \varepsilon^{-1/\tilde{s}} |\mathbf{w}|_{\ell_\tau^w}^{1/\tilde{s}}$, whereas the number of floating point operations and storage locations can be bounded by an absolute multiple of the same expression. In particular, this is possible if \mathbf{G} is s^* -compressible, which depends on the smoothness and number of vanishing moments of the wavelets, see [38, 39, 41] for a detailed discussion of this relation. Analogous properties have to be required for $\mathbf{COARSE}[\mathbf{w}, \varepsilon]$ and $\mathbf{RHS}[\varepsilon]$. From $\mathbf{u} \in \ell_\tau^w(\mathcal{I})$ and the compressibility of \mathbf{G} , it can be inferred (cf. [19]) that also $\mathbf{f} \in \ell_\tau^w(\mathcal{I})$ and $\#\text{supp } \mathbf{f}_\varepsilon \lesssim \varepsilon^{-1/s} |\mathbf{u}|_{\ell_\tau^w}^{1/s}$. Nevertheless, the feasibility of a routine $\mathbf{RHS}[\varepsilon]$, computing such an approximation in $\mathcal{O}(\varepsilon^{-1/s} |\mathbf{u}|_{\ell_\tau^w}^{1/s})$ operations, depends on the right-hand side at hand. Under these assumptions the following result can be proved, see [19].

Theorem 6.2. *Let $\mathbf{w}_\varepsilon := \mathbf{SOLVE}[\omega, \varepsilon]$, $\omega \geq \|\mathbf{Q}\mathbf{u}\|_{\ell_2}$, and let for any $s \in (0, s^*)$ the projection \mathbf{Q} onto $\text{ran}(\mathbf{G})$ be bounded on $\ell_\tau^w(\mathcal{I})$, $\tau = (s + \frac{1}{2})^{-1}$. Then, if the solution $\mathbf{u} \in \ell_\tau^w(\mathcal{I})$, $\check{\tau} = (\check{s} + \frac{1}{2})^{-1}$, for some $\check{s} \in (0, s^*)$, it is $\#\text{supp } \mathbf{w}_\varepsilon \lesssim \varepsilon^{-1/\check{s}} |\mathbf{u}|_{\ell_\tau^w}^{1/\check{s}}$. Moreover, the number of arithmetic operations and storage locations can be bounded by the same expression.*

Consequently, in view of (6.2), the method is of *asymptotically optimal complexity*.

Remark 6.3. Due to the fact that the iterates \mathbf{w}_ε of \mathbf{SOLVE} are not necessarily contained in $\text{ran}(\mathbf{G})$, i.e., in general $(\mathbf{I} - \mathbf{Q})\mathbf{w}_\varepsilon \neq 0$, in order to prove the above optimality statement, ℓ_τ^w -boundedness of \mathbf{Q} is assumed. So far this assumption has only been rigorously verified for special situations, see [20, 38, Section 4.3]. For a detailed discussion of this assumption, and ways to circumvent it, see [19, 38].

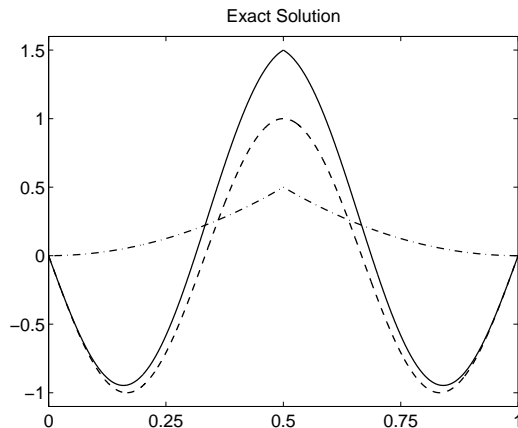


Figure 7: Exact solution (solid line) for the one-dimensional example being the sum of the dashed and dash-dotted functions.

6.2 Numerical Experiments

Poisson Equation on the Interval

We consider the variational formulation of the following problem of order 2 on the interval $\Omega = (0, 1)$, with homogeneous boundary conditions

$$-u'' = f \quad \text{in } \Omega, \quad u(0) = u(1) = 0. \quad (6.3)$$

The right-hand side f is given as the functional defined by $f(v) := 4v(\frac{1}{2}) + \int_0^1 g(x)v(x)dx$, where

$$g(x) = -9\pi^2 \sin(3\pi x) - 4.$$

The solution is consequently given by

$$u(x) = -\sin(3\pi x) + \begin{cases} 2x^2 & , x \in [0, \frac{1}{2}) \\ 2(1-x)^2 & , x \in [\frac{1}{2}, 1] \end{cases} ,$$

see Figure 7. As an overlapping domain decomposition we choose $\Omega = \Omega_1 \cup \Omega_2$, where $\Omega_1 = (0, 0.7)$ and $\Omega_2 = (0.3, 1)$. Associated with this decomposition we construct our aggregated wavelet frames just as the union of local bases on Ω_1 and Ω_2 . For this simple situation, by employing a C^∞ -partition of the unity $\{\sigma_i\}_{i=1,2}$ relative to the covering $\mathcal{C} = \{\Omega_1, \Omega_2\}$, and by applying (4.7) to the local wavelet bases $\Psi^{(1)}$ on Ω_1 and $\sigma_1 u$ and to $\Psi^{(2)}$ and $\sigma_2 u$, it is immediate to see that the representation $\mathbf{u} = D\langle u, \tilde{\Psi} \rangle_{L_2} \in \ell_2(\mathcal{I})$ of the continuous solution u with respect to the non-canonical dual frame

$$\tilde{\Psi} := \{\sigma_1 \tilde{\psi}_{(1,\mu)}\}_{\mu \in \mathcal{I}^\square} \cup \{\sigma_2 \tilde{\psi}_{(2,\mu)}\}_{\mu \in \mathcal{I}^\square}$$

is contained in $\ell_\tau^w(\mathcal{I})$, $\tau = (s + \frac{1}{2})^{-1}$, for $0 < s < d - 1$. Together with the assumed boundedness of the ℓ_2 -orthogonal projection \mathbf{Q} onto $\text{ran}(\mathbf{G})$ from Theorem 6.2, this shows that the assumption in (6.1) is indeed satisfied for $\mathbf{Q}\mathbf{u}$ and $\tau = (s + \frac{1}{2})^{-1}$, $0 < s < d - 1$.

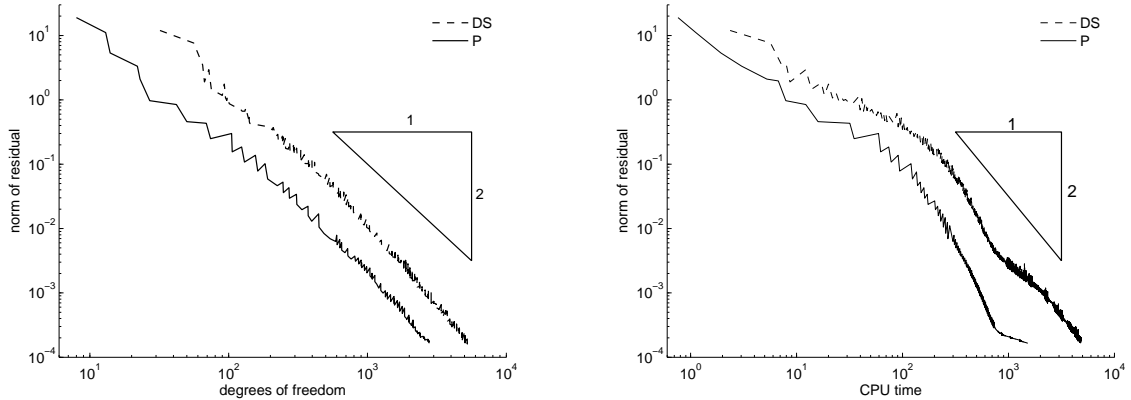


Figure 8: Convergence histories of the adaptive steepest descent method with respect to the support size of the iterates (*left column*) or CPU time (*right column*) for $d = \tilde{d} = 3$. The algorithm has been tested with aggregated frames based on interval bases from Section 5 (solid line) and [24] (dashed line).

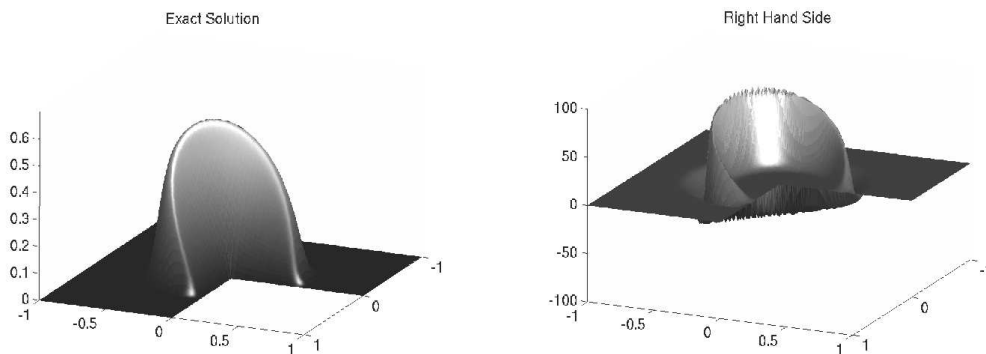


Figure 9: Exact solution (left) and right-hand side for the two-dimensional Poisson equation in an L-shaped domain.

The left diagram in Figure 8 demonstrates the decrease of the ℓ_2 -error of an iterate \mathbf{u}_ε of **SOLVE** with respect to $\#\text{supp } \mathbf{u}_\varepsilon$. Indeed, the optimal convergence rate $d - 1 = 2$ can be observed for both types of bases on the interval. Due to the smaller spectral condition number of \mathbf{G} , the basis from Section 5 performs quantitatively better. The right diagram addresses the relation between ℓ_2 -error and CPU time. Because of the generally smaller supports of the iterates and the smaller number of iterations needed, here, a remarkable discrepancy between the performances of **SOLVE** can be observed. In particular, in order to attain the same accuracy, when our new bases are employed, about ten times less CPU time is needed compared to the bases from [24].

Poisson Equation on the L-shaped Domain

Let us now consider the variational formulation of Poisson's equation in two spatial dimen-

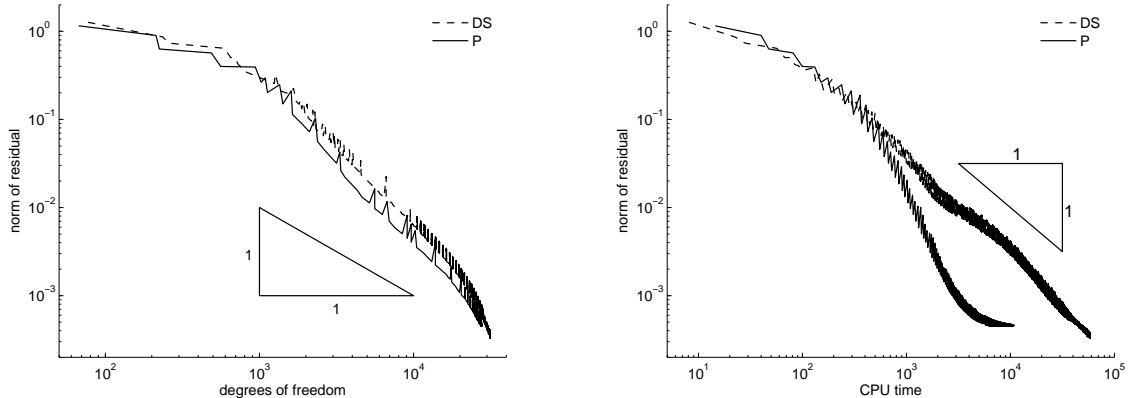


Figure 10: Convergence histories of the adaptive steepest descent method with respect to the support size of the iterates (*left column*) or CPU time (*right column*) for $d = \tilde{d} = 3$. The algorithm has been tested with aggregated frames based on interval bases from Section 5 (solid line) and [24] (dashed line).

sions:

$$-\Delta u = f \text{ in } \Omega, \quad u|_{\Omega} = 0. \quad (6.4)$$

The problem is chosen in such a way that the application of *adaptive* algorithms pays off most, as it is the case for domains with reentrant corners. As Theorem 4.8 shows, the reentrant corners themselves lead to singular parts in the solutions, forcing them to have a limited Sobolev regularity, even for smooth right-hand sides. As exact solution, we choose

$$\mathcal{S}(r, \theta) := \zeta(r)r^{2/3} \sin\left(\frac{2}{3}\theta\right),$$

which coincides with the first term of the inner sum related to the reentrant corner in (4.15) and the choice $c_{l,m} = 1$. It is shown together with the corresponding right-hand side in Figure 9. Recall from Example 4.11 that $\mathcal{S} \in H^s(\Omega)$ for $s < 5/3$ only, but it is contained in every Besov space $B_\tau^s(L_\tau(\Omega))$, where $s > 0$, $1/\tau = (s - 1)/2 + 1/2$. While the convergence rate of a uniform refinement strategy is determined by the Sobolev regularity of the solution, in the context of adaptive schemes it depends on the Besov regularity [16]. In particular, considering linear approximation with piecewise quadratic spline wavelets ($d = 3$), the best possible convergence rate in the $H^1(\Omega)$ -norm for uniform refinement strategies is $\mathcal{O}(N^{-(\frac{5}{3}-1)/2})$, with N being the number of unknowns, whereas our adaptive frame scheme gives the optimal rate $\mathcal{O}(N^{-1})$. The latter follows from Theorem 6.2 under the assumptions summarized in Section 6.1. We emphasize that property (6.1) for $s < (d - t)/n = 1$ is now covered by Theorem 4.5. Formerly, in [19], it was assumed without further investigation, but its verification has turned out to be a non-trivial problem.

For our numerical experiments, we have used an aggregated wavelet frame, corresponding to the covering $\Omega_1 = (-1, 0) \times (-1, 1)$, and $\Omega_2 = (-1, 1) \times (-1, 0)$ from Section 3.2.

In Figure 10 we have collected the convergence histories of **SOLVE** for both types of biorthogonal wavelets on the interval. Again quantitatively better results are obtained for

our new basis in terms of the degrees of freedom N and the CPU time spent.

Acknowledgements. The authors would like to warmly thank Prof. Winfried Sickel, University of Jena, for several very helpful suggestions. His courtesy definitely improved the paper. Especially, the verification of Lemma 4.9, and thus also Lemma 4.13, which form the principal ingredients to show that the theory developed in Section 4 is useful, could be realized thanks to his kind support.

References

- [1] R. A. Adams, *Sobolev Spaces*, Academic Press, New York, 1975.
- [2] A. Barinka, *Fast computation tools for adaptive wavelet schemes*, Ph.D. thesis, RWTH Aachen, 2005.
- [3] A. Barinka, T. Barsch, P. Charton, A. Cohen, S. Dahlke, W. Dahmen, and K. Urban, *Adaptive wavelet schemes for elliptic problems: Implementation and numerical experiments*, SIAM J. Sci. Comput. **23** (2001), no. 3, 910–939.
- [4] L. Borup, R. Gribonval, and M. Nielsen, *Bi-framelet systems with few vanishing moments characterize Besov spaces*, Appl. Comput. Harmon. Anal. **17** (2004), 3–28.
- [5] C. Canuto, A. Tabacco, and K. Urban, *The wavelet element method part I: Construction and analysis*, Appl. Comput. Harmon. Anal. **6** (1999), 1–52.
- [6] J. M. Carnicer, W. Dahmen, and J. M. Peña, *Local decomposition of refinable spaces and wavelets*, Appl. Comput. Harmon. Anal. **3** (1996), 127–153.
- [7] M. Charina, C. Conti, and M. Fornasier, *Adaptive frame methods for nonlinear variational problems*, (2008), to appear in Numer. Math.
- [8] C. K. Chui and E. Quak, *Wavelets on a bounded interval*, Numerical Methods of Approximation Theory (Dietrich Braess and Larry L. Schumaker, eds.), International Series of Numerical Mathematics, vol. 9, Birkhäuser, 1992, pp. 53–75.
- [9] A. Cohen, *Wavelet Methods in Numerical Analysis*, Handbook of Numerical Analysis (P.G. Ciarlet and J.L. Lions, eds.), vol. VII, North-Holland, Amsterdam, 2000, pp. 417–711.
- [10] A. Cohen, W. Dahmen, and R. DeVore, *Adaptive wavelet methods for elliptic operator equations — Convergence rates*, Math. Comp. **70** (2001), 27–75.
- [11] A. Cohen, I. Daubechies, and J.-C. Feauveau, *Biorthogonal bases of compactly supported wavelets*, Comm. Pure Appl. Math. **45** (1992), 485–560.
- [12] A. Cohen, I. Daubechies, and P. Vial, *Wavelets on the interval and fast wavelet transforms*, Appl. Comput. Harmon. Anal. **1** (1993), 54–81.

- [13] A. Cohen and R. Masson, *Wavelet adaptive method for second order elliptic problems: Boundary conditions and domain decomposition*, Numer. Math. **86** (2000), no. 2, 193–238.
- [14] G. M. Constantine and T. H. Savits, *A multivariate Faa di Bruno formula with applications*, Trans. Amer. Math. Soc. **348** (1996), no. 2, 503–520.
- [15] S. Dahlke, *Besov regularity for elliptic boundary value problems on polygonal domains*, Applied Mathematics Letters **12** (1999), 31–38.
- [16] S. Dahlke, W. Dahmen, and R. DeVore, *Nonlinear approximation and adaptive techniques for solving elliptic operator equations*, Multiscale Wavelet Methods for Partial Differential Equations (W. Dahmen, A. Kurdila, and P. Oswald, eds.), Academic Press, San Diego, 1997, pp. 237–283.
- [17] S. Dahlke, W. Dahmen, R. Hochmuth, and R. Schneider, *Stable multiscale bases and local error estimation for elliptic problems*, Appl. Numer. Math. **23** (1997), 21–48.
- [18] S. Dahlke, M. Fornasier, and T. Raasch, *Adaptive frame methods for elliptic operator equations*, Adv. Comput. Math. **27** (2007), no. 1, 27–63.
- [19] S. Dahlke, M. Fornasier, T. Raasch, R. Stevenson, and M. Werner, *Adaptive frame methods for elliptic operator equations: The steepest descent approach*, IMA J. Numer. Anal. **27** (2007), no. 4, 717–740.
- [20] S. Dahlke, K. Gröchenig, and M. Fornasier, *Optimal adaptive computations in the Jaffard algebra and localized frames*, Bericht 2006-4, FB 12 Mathematik und Informatik, Philipps-Universität Marburg, 2006, preprint.
- [21] W. Dahmen, *Multiscale analysis, approximation, and interpolation spaces*, Approximation Theory VIII (C. K. Chui, ed.), vol. 2, 1995, pp. 47–88.
- [22] ———, *Stability of multiscale transformations*, J. Fourier Anal. Appl. **4** (1996), 341–362.
- [23] W. Dahmen, A. Kunoth, and K. Urban, *Biorthogonal spline-wavelets on the interval — Stability and moment conditions*, Appl. Comput. Harmon. Anal. **6** (1999), 132–196.
- [24] W. Dahmen and R. Schneider, *Wavelets with complementary boundary conditions — Function spaces on the cube*, Result. Math. **34** (1998), no. 3–4, 255–293.
- [25] ———, *Composite wavelet bases for operator equations*, Math. Comp. **68** (1999), 1533–1567.
- [26] ———, *Wavelets on manifolds I. Construction and domain decomposition*, SIAM J. Math. Anal. **31** (1999), 184–230.
- [27] R. DeVore, *Nonlinear approximation*, Acta Numerica **7** (1998), 51–150.
- [28] P. Grisvard, *Elliptic Problems in Nonsmooth Domains*, Monographs and Studies in Mathematics, vol. 24, Pitman (Advanced Publishing Program), Boston, MA, 1985.

- [29] ———, *Singularities in Boundary Value Problems*, Research Notes in Applied Mathematics, Springer, 1992.
- [30] H. Harbrecht and R. Stevenson, *Wavelets with patchwise cancellation properties*, Math. Comput. **75** (2006), no. 256, 1871–1889.
- [31] R. Q. Jia and Q. T. Jiang, *Spectral analysis of the transition operator and its applications to smoothness analysis of wavelets*, SIAM J. Matrix Anal. Appl. **24** (2003), no. 4, 1071–1109.
- [32] A. Kunoth and J. Sahner, *Wavelets on manifolds: an optimized construction*, Math. Comp. **75** (2006), 1319–1349.
- [33] M. Primbs, *On the computation of boundary entries of Gramian matrices for refinable bases on the interval*, preprint, 2006.
- [34] ———, *Stabile biorthogonale Spline-Waveletbasen auf dem Intervall*, Dissertation, Universität Duisburg–Essen, 2006.
- [35] T. Raasch, *Adaptive wavelet and frame schemes for elliptic and parabolic equations*, Dissertation, Philipps–Universität Marburg, 2007.
- [36] T. Runst and W. Sickel, *Sobolev Spaces of Fractional Order, Nemytskij Operators, and Nonlinear Partial Differential Equations*, de Gruyter Series in Nonlinear Analysis and Applications, 1996.
- [37] L. Schumaker, *Spline Functions: Basic Theory*, Wiley, New York, 1981.
- [38] R. Stevenson, *Adaptive solution of operator equations using wavelet frames*, SIAM J. Numer. Anal. **41** (2003), no. 3, 1074–1100.
- [39] ———, *On the compressibility of operators in wavelet coordinates*, SIAM J. Math. Anal. **35** (2004), no. 5, 1110–1132.
- [40] ———, *Composite wavelet bases with extended stability and cancellation properties*, SIAM J. Numer. Anal. **45** (2007), no. 1, 133–162.
- [41] R. Stevenson and M. Werner, *Computation of differential operators in aggregated wavelet frame coordinates*, IMA J. Numer. Anal. (2007), Advance Access published on September 18; doi: doi:10.1093/imanum/drm025.
- [42] N. Weyrich, *Spline wavelets on an interval*, Wavelets and Allied Topics, 2001, pp. 117–189.

List of Figures

1	Decomposition of the boundary of Ω_1 into four segments.	11
2	Classical scale of Besov spaces governing best N -term approximation in $H^t(\Omega)$ w.r.t. wavelet bases (solid line), and the relevant scale for the case of aggregated wavelet frames (dashed line).	17
3	DeVore-Triebel diagram corresponding to the proof of Theorem 4.5.	18
4	Primal and dual scaling function for $\tilde{d} = 5$	23
5	The B-Splines B_k^2 for $k = -1, \dots, 2$	24
6	The left edge boundary functions after biorthogonalization for $\tilde{d} = 5, j = 0$	29
7	Exact solution (solid line) for the one-dimensional example being the sum of the dashed and dash-dotted functions.	36
8	Convergence histories of the adaptive steepest descent method with respect to the support size of the iterates (<i>left column</i>) or CPU time (<i>right column</i>) for $d = \tilde{d} = 3$. The algorithm has been tested with aggregated frames based on interval bases from Section 5 (solid line) and [24] (dashed line).	37
9	Exact solution (left) and right-hand side for the two-dimensional Poisson equation in an L-shaped domain.	37
10	Convergence histories of the adaptive steepest descent method with respect to the support size of the iterates (<i>left column</i>) or CPU time (<i>right column</i>) for $d = \tilde{d} = 3$. The algorithm has been tested with aggregated frames based on interval bases from Section 5 (solid line) and [24] (dashed line).	38

Stephan Dahlke, Thorsten Raasch, Manuel Werner
Philipps-Universität Marburg
FB 12 Mathematik und Informatik
Hans-Meerwein Straße
Lahnberge
35032 Marburg
Germany
email: {dahlke,raasch,werner}@mathematik.uni-marburg.de
WWW: <http://www.mathematik.uni-marburg.de/~{dahlke,raasch,werner}>

Massimo Fornasier
Program in Applied and Computational Mathematics
Princeton University
Fine Hall, Washington Road
Princeton NJ-08540-1000
email: mfornasi@math.princeton.edu
WWW: <http://www.math.princeton.edu/~mfornasi>

Miriam Primbs
IMATI CNR
Via Ferrata 1
27100 Pavia
Italy
email: Miriam.Primbs@math.uni-duisburg.de
WWW: <http://www.uni-duisburg.de/FB11/STAFF/primbs/Miriam.Primbs.html>